**Laura Orsevska**
Goulanes, Bantry, Co. Cork, P75 PX73
Lauraorsevska@gmail.com
*Approximately 2 km from the nearest proposed turbine*

12 May 2026

The Secretary
An Coimisiún Pleanála
64 Marlborough Street
Dublin 1, D01 V902

**Re: Objection to the proposed Maughanaclea Wind Farm**
**Planning Reference: ACP-324165-26 / 324165**
**Applicant: Maughanaclea Wind Farm Ltd (Enerco)**

Dear Sir or Madam,

I am writing to object to the proposed wind farm at Maughanaclea. I am not a planner and I am not a lawyer. I am a person who moved from Cork city out to the Mealagh Valley because of what this valley is — quiet, dark at night, alive with creatures, and far enough from a town for the soul to settle. That is what I came here for. That is what fourteen industrial wind turbines, each one a hundred and sixty-nine metres tall to the blade tip, will take away. I would like the Commission to read what follows and to understand that for me this is not an abstract planning matter. It is the place I have made my home.

## *What I came here for*

Goulanes sits on the southern side of the Mealagh Valley. From my home and garden, the ridgeline north of us is the dominant feature — it is the line of the horizon, the shape of the sky. The developer's own Landscape and Visual Impact Assessment at Chapter 13 confirms that the proposed turbines will sit on that ridgeline, between two hundred and twelve metres and three hundred and seventy-six metres above sea level, deliberately chosen for prominence and wind exposure. Chapter 13 §13.4.1.1.3 also confirms that the landscape I live in is classified in the Cork County Development Plan as both High Landscape Value and High Landscape Sensitivity. These are not labels I am inventing. They are the developer's own categorisations of the place where it proposes to build.

More than that: in Chapter 3 §3.2.5.2.2 of the EIAR the developer itself records that, in an earlier nineteen-turbine layout, turbines T08, T14 and T19 were removed for the express reason that they would have caused "direct landscape effects" on the adjoining High Value Landscape. So the developer accepts the principle that a High Value Landscape designation should stop turbines from

being built. It then chooses to put fourteen of them on a ridge which is itself High Landscape Value and High Landscape Sensitivity under the same Development Plan. I cannot follow that logic and I would ask the Commission not to follow it either.

Turbines of this height — again, one hundred and sixty-nine metres, more than twice as tall as The Elysian in Cork city, which is the tallest building in Cork — will dominate the view from my home, from my garden, from every walk and drive I take in this valley, and from the homes of my neighbours. Chapter 13 §13.6.5.4.1 admits that at viewpoint VP16 the turbines will consume approximately forty-four per cent of the visible horizon, roughly one hundred and fifty-seven degrees of three hundred and sixty. That is not a discreet addition to a landscape. That is the landscape being replaced.

. . .

*What will be lost — for the animals, the birds, the night sky*

There is also the question of what this will do to the animals, the birds, and the night sky — and that, for me, is the part of this proposal that distresses me most. The site is upland blanket bog, wet heath and dry heath — priority habitats listed under Annex I of the EU Habitats Directive. The developer's own Chapter 6 (Biodiversity) confirms this. It is also habitat for the pine marten, the red squirrel, the Irish hare, and lies within the catchments of the Owvane and the Mealagh rivers, which are designated sensitive catchments for the Freshwater Pearl Mussel under Statutory Instrument No. 296 of 2009. The Freshwater Pearl Mussel is one of the most critically endangered species we have. It cannot survive disturbed or silted water. The developer proposes eighteen to twenty-four months of haul roads, excavations, four borrow pits, peat handling and concrete pouring on the slopes above two such catchments. That is not a project that can be reconciled with the protection of those species.

The site has confirmed presence of Hen Harrier and Peregrine Falcon — both Annex I species under the EU Birds Directive. The White-Tailed Sea Eagle, re-introduced to West Cork at considerable public expense, has been recorded foraging in this area. The European Court of Justice has confirmed, in Commission v Ireland (Case C-418/04), that the protections owed to Annex I bird species apply outside designated Special Protection Areas as well as inside them. The NPWS specifically warned the developer in scoping that ridges above valleys are exactly where eagles use orographic lift to gain altitude. Putting fourteen rotating blades on this ridge, at the height a soaring eagle uses, is not a risk that can be designed away. I attach as Appendix A photographs of some of the protected wildlife recorded in this area, so that the Commission may see the creatures whose homes are at issue.

On the night sky: fourteen turbines at one hundred and sixty-nine metres tip height will be required to carry aviation warning lights. The Mealagh Valley is presently a near-pristine night-sky environment. I attach as Appendix B a 2024 peer-reviewed study by Bará and Lima in the Journal of Quantitative Spectroscopy and Radiative Transfer which quantifies medium-intensity turbine aviation lights as brighter than Venus up to roughly four kilometres from the turbine, and brighter than the brightest star in the night sky out to approximately ten kilometres. Aviation lighting will harm bats, owls and moths, the nocturnal life this place still supports. It will be seen from Wild Hideaways Eco Retreat — the only registered tourist accommodation premises in the Mealagh Valley, identified by name in the developer's own Chapter 5 Tourism Impact Assessment — and from the eleven other Airbnb premises which the same chapter records within five kilometres of the site. The Programme for Government 2025 commits the State to expanding Dark Sky reserves. This project foreseeably destroys a near-pristine night sky. The two cannot be reconciled.

. . .

*Health, sleep, and what fourteen turbines do to a household*

I am writing on my own behalf, but I have to speak about the health of my household. There is a member of my household whose condition can be made worse by disturbed sleep and by persistent low-frequency or modulated sound. I attach as Appendix C the 2015 peer-reviewed systematic review and meta-analysis by Onakpoya and colleagues, published in Environment International, which finds a statistically significant increase — odds ratio 2.94 — in the reporting of sleep disturbance among people exposed to wind turbine noise compared with those who are not. The same study finds significantly increased annoyance, with effects beginning at sound pressure levels of around thirty-five decibels. The chapter does not, and the developer does not, address what these findings mean for the household which actually has to live with the turbines for thirty-five years.

The noise assessment in the EIAR has not properly addressed the terrain of this valley. I attach as Appendix D the 2017 peer-reviewed paper by Van Renterghem in the Philosophical Transactions of the Royal Society, which is specifically about sound propagation from a ridge wind turbine across a valley. It is the closest available match in the published literature to the geometry of this site — turbines on a ridge above a valley containing homes. The standard ISO 9613-2 method which the developer's noise consultants use does not capture the focusing and channelling effects which Van Renterghem's modelling identifies for exactly this kind of terrain. To rely on flat-terrain methodology in a deeply incised, hilly valley is not adequate.

I raise noise formally as a ground of objection. My concerns include night-time noise, low-frequency noise, and amplitude modulation; the inadequate selection of background monitoring locations (only six locations were used to represent seventy-nine sensitive receptors, and they were selected within the predicted thirty-five decibel $L_{a90}$ contour — a circular method that excludes the very quietest places in the valley, such as eco-retreats and bed-and-breakfast properties); and the eighteen to twenty-four months of construction-phase rock breaking and possible blasting from four borrow pits, the noise from which Chapter 12 itself predicts at fifty-nine decibels $L_{aek}$ at the closest receptor for blasting and forty-eight decibels $L_{aek}$ for rock breaking, and admits will be "audible at some locations" with air overpressure that is "difficult to control". In a hill-rimmed valley like this one, rock breaking does not just travel — it echoes.

I also have to mention, with real concern, the closures of the R586 during the construction phase. The R586 is the route from this valley to Cork hospitals and to specialist medical care. Closures of the order of weeks or months on the road that connects a rural community to Cork University Hospital are not a matter that can be deferred to a traffic management plan and called "mitigated". For a household where access to a hospital may be a question of hours, this is a serious safety concern.

My home is also within range of potential shadow flicker. The EIAR shadow flicker chapter is inconsistent on its own face about how many receptors it has assessed — §5.2.3.5 and §5.3.5.3 give seventy-nine, §5.3.6 gives one hundred and two, and the receptor table itself runs to H087. Eight dwellings are admitted to be predicted to exceed the thirty-hour annual statutory threshold for shadow flicker even after a Met Éireann sunshine correction — including individual properties at seventy-three, ninety-eight and one hundred and three hours per year of predicted exposure. Mitigation is by software within the turbines themselves, for thirty-five years, on the developer's word and with no independent enforcement mechanism specified. That is not a reassurance.

. . .

### *Water, peat, and what the slope above this house is made of*

I rely on a private well. No baseline testing of private wells has been undertaken by the developer. This is true of every household in the Mealagh Valley I know of. There is no "before" against which any future contamination, turbidity or yield reduction can be measured. The proposed turbine bases, borrow pits and access tracks involve substantial excavation in peat and in steep peaty slopes. The Geological Survey of Ireland's Landslide Susceptibility Map shows the site as moderate-to-high susceptibility. There has been a documented peat slide at Goulacullin within four kilometres of this site. Once a peat slide enters a watercourse it travels for kilometres and it does not come back. Construction is to

last eighteen to twenty-four months and to involve four borrow pits, twenty-seven kilometres of cabling, and turbine foundations on slopes the developer itself describes as steep. The risk is not theoretical.

. . .

*What was here before us — the heritage of this place*

The Mealagh Valley is, by the developer's own count in Chapter 14, surrounded by an extraordinary cluster of prehistoric monuments — eleven recorded archaeological sites within the wind farm site, two hundred and ten within five kilometres, and six National Monuments within ten kilometres. The Kealkill Stone Circle, two and a half thousand years old, sits under Preservation Order PO 69/1938 and is two and a third kilometres from the proposed turbines. Chapter 14 admits, in its own words, that the visual effects on the setting of these monuments "cannot be mitigated". That is the developer's consultants saying that what they propose will permanently change how these monuments are seen and felt, and that nothing they can do will undo it. I do not think the Commission should permit a development whose own cultural heritage consultants admit cannot be mitigated.

. . .

*How this proposal has been put to the community*

The developer held its public information event for this proposal not in the valley, and not in Kealkill, but in the Westlodge Hotel in Bantry, more than nine kilometres from the site. Direct household notification reportedly extended only to a two-kilometre buffer, even though the developer's own Landscape and Visual Impact Assessment study area extends out to between five and fifteen kilometres, and the shadow flicker study area to one point three three kilometres. The consultation area is a fraction of the impact area. The Tourism Impact Assessment in Chapter 5 itself names Wild Hideaways Eco Retreat in the Mealagh Valley as the only registered tourist accommodation within five kilometres of the site — yet the developer's Community Engagement Report (Appendix 2-1) confirms that no tourism business in the valley was consulted at all. None of this gives me confidence that the developer is engaging honestly. I was not given clear information about the turbine size, the road works, or the construction phase. I had to find out from neighbours and from the EIAR itself.

This project is not community-owned. The profits leave the area. The community has not given meaningful consent to this development. A small "Community Benefit Fund", paid out of the same revenues we are being asked to surrender our valley to generate, is not consent. It is compensation — and inadequate compensation — for a transformation we did not ask for and do not want.

. . .

*A question I would like the Commission to consider*

I support climate action. I do not say that lightly — I say it because it is true. But this proposal does not present itself as climate action against doing nothing. It presents itself as climate action against the survival of irreplaceable habitat, the homes of protected species, prehistoric heritage that is two and a half thousand years old, a near-pristine night sky, and the wellbeing of every household and every animal in this valley. Better-sited alternatives — offshore wind, brownfield sites, rooftop solar at scale — do not require any of these to be sacrificed.

So the question I would like the Commission to consider is this. How can it be justified to permit a wind farm in a place that the developer itself, in its own Landscape and Visual Impact Assessment, classifies as High Landscape Value and High Landscape Sensitivity; in two Freshwater Pearl Mussel catchments; on Annex I priority habitat; on land used by Annex I bird species; in a near-pristine night-sky environment; in a tourism destination explicitly identified in Fáilte Ireland's own West Cork Coast Destination and Experience Development Plan; surrounded by six National Monuments within ten kilometres; and against the wishes of the community that lives here — when half the country produces no wind energy at all, and Cork and Kerry together already generate more than the remaining twenty-four counties combined? That is the question. I do not believe a reasoned answer can be given. I respectfully ask the Commission to refuse permission.

I would be grateful if my submission could be acknowledged in writing.

Yours faithfully,

_____

**Laura Orsevska**
Goulanes, Bantry, Co. Cork, P75 PX73
*Approximately 2 km from the nearest proposed turbine*

# APPENDICES

**Appendix A —** Photographs of protected wildlife recorded in the area: pine marten, red squirrel, Irish hare, and other Annex II / Annex IV species whose habitat is at issue.

**Appendix B —** Bará, S. & Lima, R.C. (2024). “Quantifying the visual impact of wind farm lights on the nocturnal landscape.” *Journal of Quantitative Spectroscopy and Radiative Transfer* 329, 109203.

**Appendix C —** Onakpoya, I.J., O’Sullivan, J., Thompson, M.J. & Heneghan, C.J. (2015). “The effect of wind turbine noise on sleep and quality of life: A systematic review and meta-analysis of observational studies.” *Environment International* 82, 1-9.

**Appendix D —** Van Renterghem, T. (2017). “Sound propagation from a ridge wind turbine across a valley.” *Philosophical Transactions of the Royal Society A* 375, 20160105.

# APPENDIX A

*Protected wildlife recorded in the area surrounding the proposed development*


*Pine Marten (Martes martes) — Annex V species under the EU Habitats Directive; protected under the Irish Wildlife Acts. Recorded in the area surrounding the proposed development.*


*Red Squirrel (Sciurus vulgaris) — protected under the Irish Wildlife Acts; population threatened across much of Ireland by habitat loss. Recorded in the area surrounding the proposed development.*


*Irish Hare (Lepus timidus hibernicus) — Annex V species, endemic to Ireland; protected under the Irish Wildlife Acts. Recorded by trail camera in the area surrounding the proposed development.*

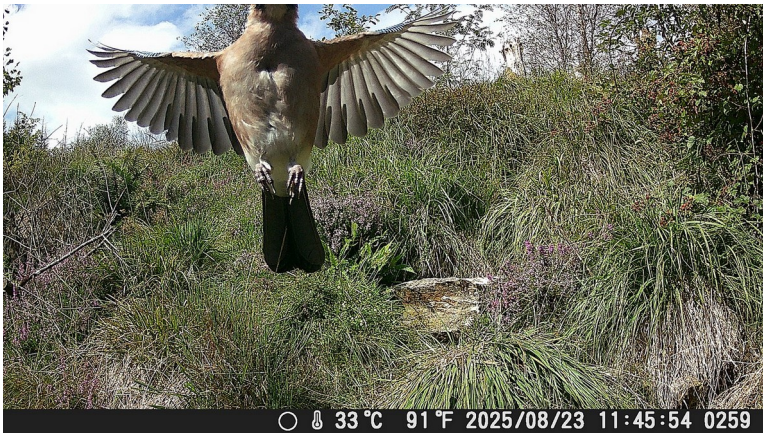


*Eurasian Jay (Garrulus glandarius) — protected under the Irish Wildlife Acts; key seed-disperser of native oak woodland. Recorded in the area surrounding the proposed development.*

Journal of Quantitative Spectroscopy & Radiative Transfer 329 (2024) 109203

Contents lists available at ScienceDirect

Journal of Quantitative Spectroscopy and Radiative Transfer

journal homepage: www.elsevier.com/locate/jqsrt

# Quantifying the visual impact of wind farm lights on the nocturnal landscape

Salvador Bará [a], Raul C. Lima [b,c,*]

[a] Former profesor titular (retired) at Universidade de Santiago de Compostela (USC), Santiago de Compostela, 15782 Galicia, Spain, European Union
[b] Física, Escola Superior de Saúde, Politécnico do Porto, Portugal
[c] IA – Instituto de Astrofísica e Ciências do Espaço, Univ Coimbra, Portugal

ARTICLE INFO

*Keywords:*
Light pollution
Wind farms
Nocturnal landscape
Environmental impacts assessment
Naked eye astronomy
Atmospheric extinction

ABSTRACT

Wind farm lights are a conspicuous feature in the nocturnal landscape. Their presence is a source of light pollution for residents and the environment, severely disrupting in some places the aesthetic, cultural, and scientific values of the pristine starry skies. In this work we present a simple model for quantifying the visual impact of individual wind turbine lights, based on the comparison of their brightness with the brightness of well-known night sky objects. The model includes atmospheric and visual variables, and for typical parameters it shows that medium-intensity turbine lights can be brighter than Venus up to ~4 km from the turbine, brighter than α CMa (the brightest star on the nighttime sky) until about ~10 km, and reach the standard stellar visibility limit for the unaided eye ($m_v = +6.00$) at ~38 km. These results suggest that the visual range of wind farms at nighttime may be significantly larger than at daytime, a factor that should be taken into account in environmental impact assessments.

## 1. Introduction

The need to reduce dependence on fossil fuels has fostered the development of renewable energy sources. This process has been accelerated in the last years due to the pressing urgence to address anthropogenic climate change and achieve higher levels of energy sovereignty. Among renewable sources, wind power energy is nowadays a crucial player.

The installation of new wind power facilities, both onshore and offshore, has not come without problems. Wind farms generate a wide range of environmental impacts [42,64], including but not limited to serious avian [30,34,50], and bat fatalities due to collisions [37,62,66,73] as well as changes in habitat use [41,67]. The sustainability of large offshore wind farms, planned or in construction, has been subjected to critical review in some recent European evaluations [20,45].

Besides their effects on biodiversity, wind farms also affect humans through the combined impacts of noise, lights (direct obstruction lights and stroboscopic effects of rotating blade shadows), and visual landscape degradation [48]. The annoyance produced by wind farm lights on neighboring communities has deserved growing attention in recent times [11,58,59,63].

The visual landscape degradation produced by wind farms has been evaluated mostly for daytime, based on turbine visibility estimates (limited by the contrast luminance thresholds in daylight) combined with different spatial aggregation metrics, see e.g. [31,36]. Comparatively less attention has been given to the deleterious effects of wind farm lights on the nighttime landscape (Fig. 1). The nightscape is an essential element of the human experience, whose cultural, social, scientific, and aesthetic values are assets of the intangible heritage of humankind [49]. As set forth by the Natural Sounds and Night Skies Division of the USA National Parks Service "a naturally dark night sky is more than a scenic canvas; it is part of a complex ecosystem that supports both natural and cultural resources" [56]. Borrowing from Rich and Longcore [61] on conservation planning, it can certainly be said that daytime landscapes are "only half the story–the daytime story".

In this work we present a model for quantifying the primary visual effect of wind farm lights on the nocturnal landscape. It is based on considering wind farm lights as artificial stars and applying to them the metrics used in visual astronomy to quantify their perceived brightness. That way they can be compared with the stars and other natural bodies present on the sky, facilitating an easy and intuitive evaluation of the disruption caused to the pristine nightscape. The model incorporates atmospheric and perceptual parameters. Although it is formulated in terms of human-based photometric (in lighting engineering language) or

* Corresponding author.
*E-mail address:* raulcpslima@ess.ipp.pt (R. C. Lima).

https://doi.org/10.1016/j.jqsrt.2024.109203
Received 12 June 2024; Received in revised form 18 September 2024; Accepted 24 September 2024
Available online 25 September 2024

visual band (in astronomical language) quantities, its generalization for arbitrary spectral distributions and observation bands is immediate. Wildlife shows a rich variety of spectral response curves [46], and several species have been reported to be able to use celestial cues, including individual stars, for orientation during the night (for a review, see [22]). The visibility model here developed provides the basic building block from which overall visual impact assessments can be derived with the help of different spatial aggregation metrics.

## 2. Methods

### 2.1. Retinal images of resolved and unresolved objects

The visual brightness of an object depends on several radiometric and anatomical factors, besides the physiological and neural ones. The basic inputs to the visual system are the photon catches of the retinal photoreceptor cells. The number of photons captured by an individual photoreceptor in each wavelength interval $[\lambda, \lambda + \Delta\lambda]$ during the time $\Delta t$ is proportional to $S(\lambda)E'(\lambda)\Delta\lambda\Delta t$, where $S(\lambda)$ is the spectral sensitivity of the photoreceptor and $E'(\lambda)$ is the spectral irradiance of the object's retinal image at the photoreceptor location. Wavelength values are here referred to vacuum. Hereafter we explicitly make reference to human eyes. However, the basic equations described below can also be applied to "camera-like" eyes of other species, many examples of which exist in nature (for a review, see [38]), by adapting the corresponding geometrical, optical, and spectral sensitivity parameters.

The spectral irradiance is defined as the radiant flux (photons·s$^{-1}$) per unit surface and unit wavelength interval, and is measured in photons·s$^{-1}$·m$^{-2}$·nm$^{-1}$. The spectral irradiance $E'(\lambda)$ at each retinal location can be approximately described by:

$$E'(\lambda) = T_e(\lambda)\, L(\lambda)\, \Omega \frac{A_p}{A_i} \cos\theta \tag{1}$$

where $T_e(\lambda)$ is the spectral transmittance of the ocular media (unitless), $L(\lambda)$ is the object radiance (photons·s$^{-1}$·m$^{-2}$·sr$^{-1}$·nm$^{-1}$), $\Omega$ is the solid angle (sr) subtended by the object as seen from the observer, $A_p$ is the area of the input pupil of the eye (m$^2$), $A_i$ is the area of the retinal image (m$^2$), and $\theta$ is the angle between the direction in which the object lies and the line perpendicular to the eye pupil. Eq. (1) can be equivalently rewritten in terms of $E(\lambda) = L(\lambda)\Omega\cos\theta$, the spectral irradiance produced by the object on the eye pupil, as:

$$E'(\lambda) = T_e(\lambda)\, E(\lambda)\, \frac{A_p}{A_i} \tag{2}$$

In a perfect imaging system, according to geometrical optics, the image would be an exact scaled replica of the object. The area of the image would be proportional to the solid angle subtended by the object, $\Omega$, such that $A_i = \kappa\Omega$, being $\kappa$ a constant (units m$^2$) independent from the object. For a perfect imaging system, then, the object feature that determines the input to the photoreceptor cells is its spectral radiance, $L(\lambda)$, since the solid angle $\Omega$ cancels out in Eq. (1):

$$E'(\lambda) = T_e(\lambda)\, L(\lambda)\, \frac{A_p}{\kappa} \cos\theta \tag{3}$$

and the remaining factors only depend on the eye.

Human eyes, however, are not perfect optical instruments. The eye optics deforms the ideal images to a bigger or lesser extent due to diffraction by the finite size of the eye pupil [13], refractive errors including both classical ametropies and high-order optical defects [15,28,43,44,47,53,54,55,60,69,70], and intraocular scattering due to small-scale inhomogeneities of the eye media [8,71,72]. The retinal image in a real eye is no longer an exact scaled replica of the object itself.

The actual image of an object on the human retina is given by the two-dimensional convolution of the ideal geometric image with the point-spread function of the eye, PSF [25]. The PSF is the function that describes how the eye optics deforms the image of an ideal point source. Human eyes present a high variability of PSF sizes and shapes. This convolution gives rise to a new irradiance distribution that combines the features of the convolved functions. The retinal image can be interpreted as a 'blurred' version of the perfect geometrical image, in which each point has been replaced by a PSF proportional to the object radiance at that point and the resulting irradiances have been added up.

In the limiting case of *well resolved objects*, that is, when the angular size of the object is much larger than the angular size of the PSF, the result of the convolution is a slightly blurred version of the ideal geometrical image, and Eq. (3) still approximately applies.

Conversely, when the angular size of the object viewed by the observer is substantially smaller than the angular size of the eye's PSF, as it happens e.g. with a star or distant streetlight, the retinal image is essentially equal to the PSF itself. In such cases, one may speak of *unresolved objects*. The retinal images of unresolved objects located in different directions of the central visual field are just replicas of the PSF centered in different retinal points. All these images have the same shape and size, only differing in brightness [4,54,55].

This result has important visual consequences. One of them is that the main physical factor determining the perceived brightness of an unresolved object is not the intrinsic object's radiance, as in the well-resolved case, but the irradiance $E(\lambda)$ it produces on the eye pupil. This happens because the area of the retinal image is no longer proportional to the object's solid angle, as in case of a perfect system ($A_i =$

**Fig. 1.** Nigthtime landscape with wind farm obstruction lights in Miranda do Corvo, Serra da Lousã, Portugal (40°02′42.98″N, 8°16′30.84″ W). Image credit: Raul C. Lima.

κΩ), but it is constant and equal to the area of the PSF, $A_i = A_{PSF}$. For an unresolved object Eq. (2) becomes:

$$E'(\lambda) = T_e(\lambda)\ E(\lambda)\ \frac{A_p}{A_{PSF}} \tag{4}$$

in which the object intervenes through $E(\lambda)$, since the remaining factors depend only on the eye.

The pupil size depends, among other factors, on the ambient light level and the age of the observer, with large variability between individuals [40]. The PSF size, which also shows large inter-individual variability in healthy eyes due to the differences in uncompensated ametropies, high-order eye refractive defects, and intraocular scattering commented above, depends on a non-monotonic way on the pupil size. Diffraction makes the PSF size to increase when the pupil size decreases, being dominant for pupils smaller than ~2 mm diameter; the contribution of the residual uncompensated ametropies, higher-order defects and intraocular scattering, in turn, varies in the opposite way, typically determining the PSF size for pupils of diameter ~4 mm and larger. Consequently, the best optical quality in healthy human eyes is usually achieved with pupils in the range of 2–3 mm diameter. For graphical depictions of actual PSFs see [5,54,55].

In terms of human visual (photometric) quantities, the irradiances and radiances outside the eye correspond to illuminances and luminances, respectively. The illuminance $E_v$, measured in lux (lx), is the integral over wavelengths of the spectral irradiance $E(\lambda)$ weighted by the photopic luminous efficiency function $V(\lambda)$ and multiplied by the luminous efficacy constant 683 lm/W [16]. The luminance $L_v$, measured in candela per square meter (cd·m$^{-2}$), is the analogous integral applied to the spectral radiance $L(\lambda)$. The cd is the unit of luminous intensity, $I_v$ (1 cd = 1 lm·sr$^{-1}$), being the only basic unit of the International System [10] whose definition is strictly tied to human visual perception. The cd links perceptual to physical stimuli, and by its own definition it takes implicitly into account the transmittance of the ocular media, $T_e(\lambda)$, the spectral sensitivity of the photoreceptors, $S(\lambda)$, and the basic neural processes related to the perception of luminance.

### 2.2. Illuminance produced by wind turbine lights on the eye pupil of the observer

The illuminance $E_v$ produced by an unresolved wind turbine light on the eye pupil of an observer located a distance $r$ away is:

$$E_v(r,\theta) = T_0(r)\ I_v(\alpha)\ \frac{\cos\theta}{r^2} \tag{5}$$

where $T_0(r)$ is the transmittance of the atmosphere between the wind farm light and the eye, $I_v(\alpha)$ is the luminous intensity of the wind turbine light sent towards the observer, being α the direction in which the observer is located as seen from the turbine, and θ is the angle between the normal to the pupil and the direction where the wind turbine light is located as seen from the observer. This equation, published in simplified form by Allard one and a half century ago [2,14] stems from the basic definition of these photometric quantities and the properties of light propagation in attenuating media. The formulation of Eq. (5) in terms of the luminous intensity of the wind turbine lights $I_v$ is particularly useful, because this is the photometric quantity specified for the different types of obstruction lights in the ICAO recommendations [32], and whose values have been generally adopted by the wind farm legislations, e.g. AESA [1].

For light propagation paths at angles close to the horizontal, and direct visual fixation on the turbine light (θ = 0°, cosθ = 1), Eq. (5) becomes

$$E_v(r) = I_v\ \frac{e^{-kr}}{r^2} \tag{6}$$

where $I_v = I_v(\alpha)$, and the atmospheric transmittance $T_0(r)$ is described by the Bouger-Lambert exponential law $T_0(r) = e^{-kr}$, being $k$ the combined molecular and aerosol attenuation coefficient per unit length (m$^{-1}$) at the average altitude above sea level of observer and lights.

### 2.3. How bright are wind turbine lights compared to the stars and planets of the natural sky?

The visual brightness of the stars and other unresolved point-like sources on the sky is commonly reported in astronomy in terms of "astronomical magnitudes". The astronomical magnitude is a negative logarithmic scale for expressing the in-band irradiance produced by a star, relative to some reference irradiance. This scale was qualitatively introduced by Hipparchus (c. 190–c. 120 BCE) and formalized in the 19th century [57]. The magnitude scale is also applied to illuminances $E_v$, taking as traditional reference the illuminance produced by the star Vega (α Lyr) at the top of the terrestrial atmosphere, $E_{v,ref} = E_{v,Vega} = 2.54 \times 10^{-6}$ lx [3,6,7]. According to the basic definition of this scale, an unresolved celestial object producing an illuminance $E_v$ (in lx) at the top of the terrestrial atmosphere has a visual magnitude $m_v$ given by

$$m_v = -2.5\log_{10}\left(\frac{E_v}{E_{v,ref}}\right) \tag{7}$$

Conversely, the illuminance at the top of the atmosphere in terms of the magnitude is

$$E_v = E_{v,ref}\ \times 10^{-0.4\ m_v}\ \ (\text{lx}) \tag{8}$$

It is conventionally but somehow arbitrarily accepted that an average observer may detect stars up to $m_v \approx 6.0$. As a matter of fact, the limiting visual magnitude of the unaided eye depends on many factors, including the luminance contrast threshold of the observers at the luminance adaptation level they are experiencing, the state of the atmosphere, and the artificial skyglow and glare (two effects of light pollution) at the observer location. For a detailed analysis see [8,17,65].

When a star is observed from the ground, its extra-atmospheric illuminance is reduced due to the attenuation undergone by the light rays along their path through the whole atmosphere. This can be accounted for by an atmospheric transmittance term

$$T_{atm}(z) = \exp\{-M(z)\ \tau\} \tag{9}$$

where $z$ is the angle from the star to the zenith, $\tau$ is the atmospheric vertical optical depth, and $M(z)$ is the air mass number. The atmospheric optical depth is given by $\tau = \tau_m + \tau_a$, where $\tau_m$ and $\tau_a$ are the molecular (MOD) and aerosol (AOD) optical depths, respectively, defined in terms of the corresponding vertical profiles of the molecular $k_m(h)$, and aerosol, $k_a(h)$, extinction coefficients [35] as:

$$\tau_i = \int_{h=0}^{\infty} k_i(h)\ dh\ ,\ \ i \in \{m, a\} \tag{10}$$

For an exponential atmosphere in which $k_m$ and $k_a$ decrease exponentially with the altitude $h$, with scale heights $H_m$ and $H_a$, respectively, we have

$$\tau_i = \int_{h=0}^{\infty} k_i(0)\ e^{-h/H_i}\ dh = k_i(0)\ H_i\ ,\ \ i \in \{m, a\} \tag{11}$$

being $k_i(0)$ the value of the attenuation coefficients at ground level. Typical values for the exponential scale heights are $H_m = 8$ km and $H_a$=1.5 km. The value of $\tau_m$ at sea level at the center of the visible spectrum is about 0.09–0.11, see [68] for detailed expressions, and the aerosol optical depth $\tau_a$ may range typically from 0.1 or smaller for clear atmospheres to 0.5 and larger for more turbid ones, being able to reach much higher values [19,24,29]. Note that the coefficient $k$ appearing in Eq. (6) can be written as

$$k = k_m(0) + k_a(0) = \frac{\tau_m}{H_m} + \frac{\tau_a}{H_a} \quad (12)$$

Regarding the airmass factor, for zenith angles not extremely close to the horizon its value can be calculated as $M(z) = 1/\cos z$. The number of air masses increases very quickly at angles close to the horizon, for which more accurate expressions shall be used [33]. For the zenith, $M(0^\circ) = 1$.

The atmospheric transmittance in Eq. (9) can be expressed as an equivalent extinction value $m_{ext}(z)$in magnitudes. The magnitude $m_v(z)$ of a star observed from ground at a zenith angle $z$ (angle above the horizon $90^\circ - z$) is:

$$m_v(z) = -2.5\log_{10}\left[\frac{T_{atm}(z)\ E_v}{E_{v,ref}}\right] = -2.5\log_{10}\left(\frac{E_v}{E_{v,ref}}\right) - 2.5\log_{10}[T_{atm}(z)] \quad (13)$$

that can be rewritten as

$$m_v(z) = m_v + m_{ext}(z) \quad (14)$$

being $m_v$ the extra-atmospheric magnitude given by Eq. (7), and $m_{ext}(z)$ the extinction term $m_{ext}(z) = 2.5M(z)\tau\ \log_{10}(e)$. Recall that larger (= more positive) values of $m_v(z)$ correspond to dimmer objects, due to the negative sign of the log scale magnitude definition.

The brightness of the wind farm lights can also be expressed in astronomical magnitudes, allowing that way comparing them with the natural stars. This could be done in a naïve way by directly applying Eq. (7) to the illuminance produced by the lights on the observer's eye pupil, $E_v(r)$, given in Eq. (6). There is, however, an issue that shall be kept in mind. Whereas the astronomical magnitudes refer to the irradiance produced by a celestial object *at the top* of the atmosphere, the light from wind farms reaches the observer after propagating some finite distance nearly horizontally *at the bottom* of the atmosphere. Furthermore, the brightness of a star seen from ground is not constant, but depends on its altitude above the horizon, or, equivalently, on its corresponding zenith angle $z$ as set forth in Eq. (13). Comparing the visual appearance of wind farm lights with the appearance of stars requires choosing first a reference altitude above the horizon at which the comparison stars are seen.

Once the reference zenith distance $z$ is chosen, one can easily assign to the wind farm light the extra-atmospheric magnitude $m_v$ of a star whose brightness at this $z$ would be the same as the brightness of the wind farm light perceived by the observer. According to Eqs. (6) and (7) this magnitude is:

$$m_v = -2.5\log_{10}\left[\frac{I_v\ e^{-kr}}{r^2\ T_{atm}(z)\ E_{v,ref}}\right] \quad (15)$$

Note that the transmittance $T_{atm}(z)$ is in the denominator, since we are calculating the extra-atmospheric irradiance that would result in the irradiance $E_v(r)$ at ground level after propagating through the atmosphere at a zenith angle $z$. This can alternatively be interpreted as using a reduced $T_{atm}(z)E_{v,ref}$ reference illuminance for establishing the 'zero point' of a new magnitude scale defined on irradiances at ground level, not at the top of the atmosphere.

Regarding the choice of $z$, comparing the wind farm lights with stars at the zenith (altitude $90^\circ$, $z = 0^\circ$, $M(0^\circ) = 1$) is always an option, although to perform in practice this comparison the observers should successively direct their gaze horizontally to the wind farm and vertically to the zenith sky, because the possibility of simultaneous viewing (although theoretically possible, given the size of the monocular field of view of the human eye along the vertical axis, $\sim 60^\circ$ upward and $\sim 75^\circ$ downward) would require that both light sources were imaged in diametrally opposed locations of the peripheral retina. Comparing wind farm lights with stars at the horizon would neither be a practical choice, since the attenuation of starlight in that direction is usually extremely high excepting for very clear atmospheres ($\tau \ll 0.05$), due to the large number of air masses, $M(90^\circ) \approx 38$ [33]. For instance, for $\tau = 0.2$ the extinction at the horizon is of order $m_{ext}(90^\circ) = +8.25$ magnitudes. For our present purposes an intermediate altitude above the horizon, well within the visual field of an observer looking horizontally at the lights, is appropriate. For the following sections we will use a reference altitude of $30^\circ$ ($z = 60^\circ$, $M(60^\circ) = 2.0$). The conversion of our results for other possible choices of the altitude above the horizon of the comparison stars is immediate.

## 3. Results

Fig. 2 shows the equivalent top-of-the-atmosphere (TOA) astronomical magnitude $m_v$ of a wind farm light (for a reference altitude of $30^\circ$ degrees above horizon, $z = 60^\circ$, $M(60^\circ) = 2.0$), as a function of the distance to the viewer, $r$. The atmospheric parameters are $\tau_m = 0.10$, $\tau_a = 0.20$, $H_m = 8000$ m and $H_a = 1500$ m. The results were calculated for nighttime obstruction lights of medium-intensity, $I_v = 2000$ cd, and for two levels of low-intensity, $I_v = 200$, and $I_v = 40$ cd [1,32]. The extinction coefficient at ground level is $k = 1.46 \times 10^{-4}$ m$^{-1}$, corresponding to a daytime visual range of ~26 km. The horizontal lines show the astronomical magnitudes in the Johnson-Cousins V band [9] of several conspicuous objects on the sky, namely the Moon, $m_v = -12.73$ (full Moon at mean distance from Earth, near opposition but not including the opposition surge, [3] p. 144), Venus, $m_v = -4.22$ (mean magnitude of Venus at maximum elongation, [3] p. 144), and the star Sirius (α CMa), $m_v = -1.45$ ([3] p. 240). The standard human star visibility limit with the unaided eye, $m_v = +6.00$, is also shown. In the Johnson-Cousins V band the magnitude of the star Vega (α Lyr) is usually set at $m_v = +0.03$. Fig. 2(a) shows the magnitude values within the 0.01–50 km distance range, whereas Fig. 2(b) shows an enlarged view of the first 5 km from the lights.

It can be seen in Fig. 2 that the nighttime lights of $I_v = 2000$ cd widely used in wind turbines of height between 100 and 150 m [1] can be brighter than Venus up to 4 km from the turbine, brighter than α CMa up to about 10 km, and reach the visibility limit $m_v = +6.00$ at 38 km. These results suggest that the visual range of wind farms at nighttime in pristine sites (limited by the luminous intensity of the lamps and the atmospheric attenuation) may be significantly higher than at daytime (limited by the luminance contrast thresholds applied to sunlight scattered into the line of sight [12]).

Fig. 3 shows the magnitudes $m_v$ for lights of constant luminous intensity ($I_v = 2000$ cd) and three different aerosol optical depths, $\tau_a = 0.1$, 0.2 and 0.3, corresponding to daytime visual ranges of 49 km, 26 km, and 18 km, respectively, the remaining parameters being the same as in Fig. 1. During the first kilometers from the lamps the change in visual magnitude is dominated by the geometrical factor $1/r^2$ in Eq. (15), with little influence of the horizontal-path atmospheric attenuation $e^{-kr}$, so the $m_v$ curves for different AOD are very close to each other. As the distance increases, the horizontal atmospheric attenuation becomes dominant and the values of $m_v$ increase almost linearly with $r$. The overall behavior is also function of the value of $T_{atm}(z = 60^\circ)$, the atmospheric attenuation for an equivalent star seen at $30^\circ$ above the horizon (here, two air masses), the reason behind the fact that the curves do not fully overlap in the first few km from the sources.

Fig. 4 shows the horizontal ground illuminance (in lx) produced by a single light of intensity 2000 cd located on a nacelle at 115 m above ground, with isotropic angular emission, and under the same atmospheric conditions as in Fig. 2. This illuminance is calculated using Eq. (5), by reinterpreting the angle θ as the zenith angle of the light source seen from the observer location. The constant, dotted line corresponds to the illuminance produced by a typical moonless starry sky in conditions of astronomical night, ~0.001 lx [51,52]. It can be seen that the horizontal ground illuminance produced by this mid-intensity light surpasses that of the moonless starry sky within the first 580 m from the base of the turbine, becoming two orders of magnitude smaller at a distance of 2.5 km. Recall that, unlike the retinal illuminances of non-overlapped lights perceived as individual objects, the ground

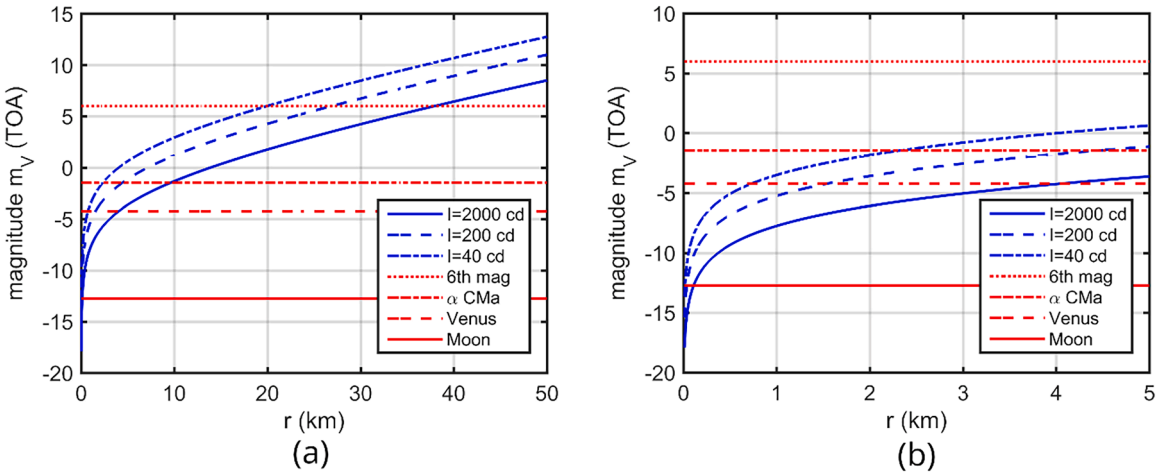


**Fig. 2.** Equivalent top-of-the-atmosphere (TOA) astronomical magnitude $m_v$ of wind turbine lights seen from distances $r$, Eq. (15), for lamps of luminous intensities $I_v$ = 2000, 200, and 40 cd, and an atmosphere with AOD $\tau_a$ = 0.2 (see text for details). (a) range 0.01–50 km, (b) enlarged view of the range 0.01–5.0 km.

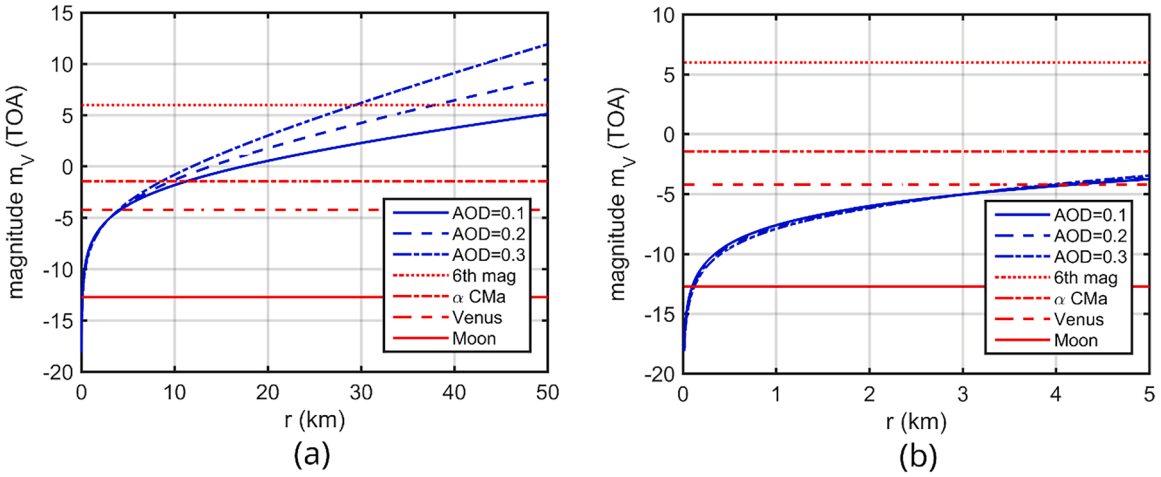


**Fig. 3.** Equivalent top-of-the-atmosphere (TOA) astronomical magnitude $m_v$ of wind turbine lights seen from distances $r$, Eq. (15), for lamps of luminous intensity $I_v$ = 2000 cd and atmospheres with AODs $\tau_a$ = 0.1, 0.2, and 0.3 (see text for details). (a) range 0.01–50 km, (b) enlarged view of the range 0.01–5.0 km.

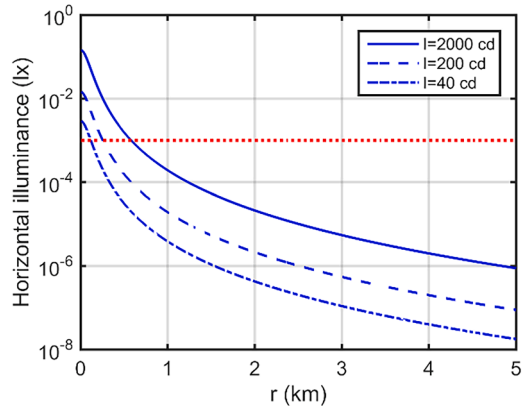


**Fig. 4.** Horizontal ground illuminance (in lx) produced by a single light of intensity 2000 cd located on a nacelle at $h_n$ =115 m above ground, with isotropic angular emission and under the same atmospheric conditions as in Fig. 2. The horizontal, dotted line corresponds to the illuminance produced by a typical moonless starry sky in conditions of astronomical night, ~0.001 lx. The variable $r$ in this figure corresponds to the horizontal distance from the base of the turbine, such that the total distance from the lamp to the ground observation point is $(r^2 + h_n^2)^{1/2}$.

illuminance produced by several lights is accumulative, hence the total ground illuminance at any point in the neighborhood of a wind farm shall be calculated as the sum of the contributions of all lamps. The direct luminous intensity of a single lamp, however, elicits significant visual responses up to much longer distances (see Fig. 2 and 3, and Section 4).

The fraction of territory within the visual range from which the windfarm lights can be seen depends on the local topography and on the height of the lights above ground level. While in flat areas the direct line of vision may be mostly unblocked across wide spans of territory, in mountainous regions it is generally limited by shadowing effects. However, since windfarms tend to be located on the highest elevations of mountain ridges, this fraction is generally very large. An example of the latter is shown in Fig. 5, where the visibility maps of four windfarm projects in the Eastern Mountains of Galicia (historic nationality and autonomous community in the kingdom of Spain, European Union) are displayed as graylevel rasters with the number of wind turbines from each windfarm that can be seen from each pixel. The red lines around each windfarm show the 4 km, 10 km, and 38 km range areas. These four windfarms are located relatively close to each other. Each one has particular visibility impacts, but the affected fraction of territory is in all cases remarkable. Their aggregated effect is shown in Fig. 6, at a spatial scale that allows discerning the variable but widespread visual impacts

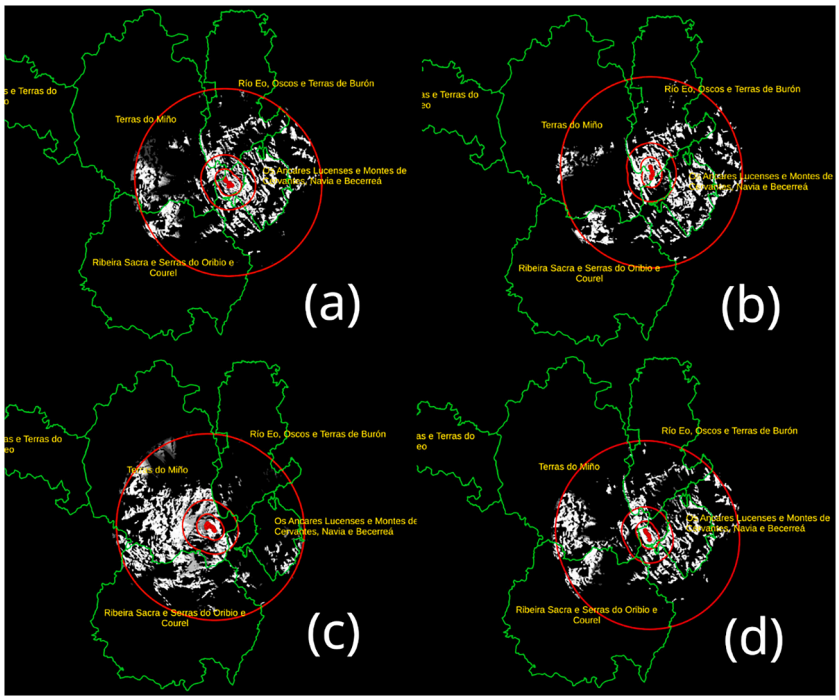


**Fig. 5.** Visual territorial impact of four windfarm projects in Galicia (kingdom of Spain, European Union). Project names, number of wind turbines (*N)* and nacelle heights ($h_n$): (a) Chao do Marco, $N = 8$, $h_n$ =115 m; (b) Monteiro, $N = 8$, $h_n$ =107 m; (c) Reboiro, $N = 11$, $h_n$ =121 m; (d) Serra do Furco, $N = 7$, $h_n$ =115 m. Graylevels indicate the number of wind turbines of each windfarm that can be seen from each pixel (from 0 to *N)*. The red lines around each windfarm show the 4 km, 10 km, and 38 km range areas. The green borders show the limits of the surrounding Biosphere Reserves (clockwise, from the upper left, "Mariñas Coruñesas e Terras do Mandeo", "Terras do Miño", "Río Eo, Oscos e Terras de Burón", "Os Ancares Lucenses e Montes de Cervantes, Navia e Becerreá", and "Ribeira Sacra e Serras do Oribio e Courel". Shp layer copyright: management boards of the Reserves). Digital elevation model PNOA_MDT200_ETRS89_HU29 (Galicia) (PNOA 2010–2013 CC-BY scne.es). Maps elaborated with QGIS ver. 3.22.10-Białowieża (https://qgis.org/).

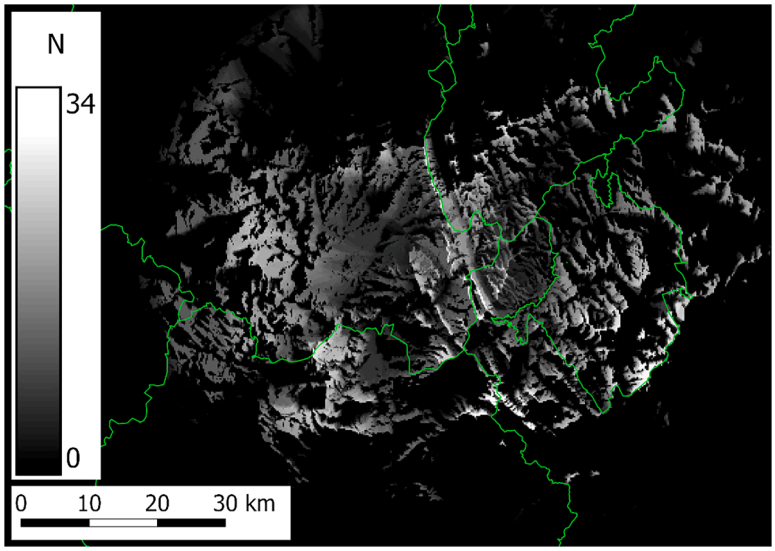


**Fig. 6.** Aggregated visibility map of the four wind-farm projects displayed in Fig. 5. The grayscale indicates the total number *N* of wind turbine nacelles seen from each location.

across these Biosphere Reserves region.

## 4. Discussion

The results obtained using the main equation of this work, Eq. (15), show that wind turbine lights can compete with natural sky objects up to distances in the range of tens of km. This has a non-negligible effect on the nocturnal landscape, particularly so because these lights are normally seen close to the horizon, towards which very often the human direction of gaze is oriented.

The calculations were made under some simplifying assumptions and can be generalized without difficulty to account for additional factors, as e.g. the relative and absolute altitudes above sea level of observers and lights (here assumed to be equal), the change of the luminous intensity of the wind farm lamps with the emission angle, or the spectral dependence of the conversions between Johnson-Cousin V magnitudes and

luminances. Also, we have assumed photopically adapted observers (that is, observers who are looking at the lights from windows of lit spaces indoors, or shortly after leaving illuminated areas outdoors). The calculations for mesopic or scotopic adaptation states can be easily done if some additional information about the wind farm light spectra is available, see e.g. [7,23].

In Section 3 it has been implicitly assumed that, although each wind turbine light is seen as an unresolved object, different lights are enough separated angularly among themselves as to ensure that the corresponding PSFs do not significantly overlap in the observer's retina. The objects can then be perceived independently, the attention may shift from one to another [39], the detection thresholds remain unaltered [27], and their magnitudes $m_v$ are correctly described by Eq. (15) using the $I_v$ of each individual lamp. However, on some occasions several distant lights may happen to be angularly very close, as seen from the observer, such that their PSFs substantially overlap in the retina. In that case they would appear as a single and brighter (but still unresolved) object, and its resulting magnitude $m_v$ shoud be calculated by adding first the iluminances $E_v(r)$ produced by each lamp on the eye pupil, Eq. (6), taking into account their possibly different distances and luminous intensities, and then applying Eq. (15) to the total $E_v(r)$resulting from this sum.

As shown in Section 3, the distance range of the disruptive effects of wind-farm lights is different if expressed in terms of the ground illumination (horizontal illuminance) or in terms of visual perception of the lights (retinal image brightness). Whereas the horizontal illuminance is comparable to or larger than the one produced by the natural moonless starry sky up to distances of a few hundred meter (580 m for 2000 cd lamps), the visual brightness of the lamps competes with the dimmest visible stars of the night sky up to several tens of km (38 km, for the same type of lamps). This difference in range is not unexpected. It is mainly due to the focusing ability of the eye, which concentrates the flux from the pupil illuminance onto a small region of the retina (equal to the eye PSF, for an unresolved light source), proportionally increasing the illuminance on the retinal photoreceptors and hence their photon catches. The retinal images of the lights, then, act as conspicuous visual stimuli even at long distances, and may have attracting or disorienting effects in species that navigate based on cues provided by localized light sources. The horizontal illuminance, in turn, is instrumental for the visual perception of the ground, and the threats and opportunities present on it.

The basic model presented in this work allows for an easy quantification of the visual impact of individual wind farm lights on the nocturnal landscape, by direct comparison of their brightness with the brightness of conspicuous objects of the pristine starry sky. This visibility model is based on well-known first principles, and the results presented here correspond to average atmospheric conditions. The application to observations in field conditions is under way. The main metrological challenge lies in the accurate determination of the aerosol content of the atmosphere at the moment of observation. Whereas daytime data on aerosols are widely available, reliable nighttime data are considerably more scarce.

An issue that has not been addressed here and that deserves further consideration is the quantification of the visual aggregated impact of high numbers of wind farm lights shining simultaneously across large stretches of the horizon, a not uncommon situation in areas with very high density of turbines. Metrics developed for quantifying aggregated visual impacts during daytime [31,36] offer some interesting starting points. Besides its direct application to landscape assessment, it may be of potential interest for professional astronomy, whose ground-based observatories are subjected to an increasing stress by the presence and effects of artificial lights [21,26].

This paper dealt with the quantitative evaluation of the visual effects of wind farm lights, without delving into a detailed discussion of the remediation measures that could be adopted. This discussion requires a comprehensive, broader social approach that deserves a specific work. Classical technological adaptations may not be sufficient nor, in many cases, applicable. Unlike public streetlamps, which are designed to illuminate public spaces but do not require to be seen themselves, the wind-farm light beacons are purposely installed to be seen from long distances in a broad range of directions. This precludes in principle the use of lamp shielding approaches that have been shown to be very useful for reducing the ecological impact of street luminaires [18].

## 5. Conclusions

Wind farm lights are a source of light pollution in the nocturnal landscape. In this work we quantify the impact of individual light sources by comparing their perceived brightness with the brightness of the stars and other conspicuous bodies of the starry night sky. For typical parameters of the lights and the atmosphere our model shows that medium-intensity turbine lights can be brighter than Venus up to ~4 km distance, brighter than α CMa (the brightest star on the nighttime sky) up to about ~10 km, and reach the standard stellar visibility limit for the unaided eye ($m_v = +6.00$) at ~38 km. These results suggest that the visual range of wind farms at nighttime may be considerably larger than at daytime. This factor should be taken into account in environmental impact assessments.

## CRediT authorship contribution statement

**Salvador Bará:** Writing – original draft, Software, Methodology, Investigation, Formal analysis, Data curation, Conceptualization. **Raul C. Lima:** Software, Validation, Writing – review & editing.

## Declaration of competing interest

The authors declare that they have no known competing financial interests or personal relationships that could have appeared to influence the work reported in this paper.

## Data availability

No data was used for the research described in the article.

## Acknowledgments and AI disclaimer

No AI tools have been used in this work.

## References

[1] AESA – Agencia Estatal de Seguridad Aérea. Guía de Señalamiento e Iluminación de Turbinas y Parques Eólicos. https://www.seguridadaerea.gob.es/sites/default/files/ssaa-17-gui-126-a01.pdf; 2017 [accessed 2 September 2023].
[2] Allard É. Mémoire sur l'intensité et la portée des phares. Paris, France: Imprimerie Nationale; 1876. p. 74.
[3] Allen CW. Astrophysical quantities. 3rd ed. London: Athlone Press; 1973.
[4] Bará S. The sky within your eyes (Eye aberrations and visual Astronomy). Sky Telescope 2013;126(2):68–71.
[5] Bará S. Naked-eye Astronomy: optics of the starry night skies. In: Proc. SPIE 9289, 12th Education and Training in Optics and Photonics Conference; 2014. 92892S. https://doi.org/10.1117/12.2070764.
[6] Bará S. Variations on a classical theme: on the formal relationship between magnitudes per square arcsecond and luminance. Int J Sustain Light 2017;19(2): 104–11. https://doi.org/10.26607/ijsl.v19i2.77.
[7] Bará S, Aubé M, Barentine J, Zamorano J. Magnitude to luminance conversions and visual brightness of the night sky. Mon Not R Astron Soc 2020;493:2429–37. https://doi.org/10.1093/mnras/staa323.
[8] Bará S, Bao-Varela C. Skyglow inside your eyes: intraocular scattering and artificial brightness of the night sky. Int J Sustain Light 2023;25(1):1–9. https://doi.org/10.26607/ijsl.v25i01.130.
[9] Bessell MS. UBVRI Passbands. Publ Astron Soc Pac 1990;102:1181–99. https://doi.org/10.1086/132749.
[10] BIPM Proceedings of the 26th meeting of the General Conference on Weights and Measures (2018). Sèvres, France: Bureau international des poids et mesures; 2019, p. 472. https://doi.org/10.59161/CGPM2018RES1E.

[11] Bjørn S, Lyhne I, Philipp D, Nedergaard H, Tolnov L, Kirch J. Do demand-based obstruction lights on wind turbines increase community annoyance? Evidence from a Danish case. Renew. Energy 2022;192:164–73. https://doi.org/10.1016/j.renene.2022.04.127.
[12] Bohren CF, Clothiaux EE. Fundamentals of atmospheric radiation. Berlin: Wiley-VCH; 2006. p. 415–6. https://doi.org/10.1002/9783527618620.
[13] Born M, Wolf E. Principles of optics. 7th ed., 1999. Cambridge, UK: Cambridge University Press; 1999. p. 439–43.
[14] Bullough JD. Aviation signal lighting: impacts of lighting characteristics on visibility. Adv Appl Sci Res 2011;2:16–27.
[15] Castejón-Mochón JF, López-Gil M, Benito A, Artal P. Ocular wave-front aberration statistics in a normal young population. Vis Res 2002;42:1611–7.
[16] CIE – Commision Internationale de l'Éclairage. CIE 1988 2° Spectral luminous efficiency function for photopic vision, CIE 86:1990. Vienna: bureau Central de la CIE; 1990.
[17] Cinzano P, Falchi F. Toward an atlas of the number of visible stars. J Quant Spectrosc Radiat Transf 2020;253:107059.
[18] Dietenberger M, Jechow A, Kalinkat G, et al. Reducing the fatal attraction of nocturnal insects using tailored and shielded road lights. Commun Biol 2024;7:671. https://doi.org/10.1038/s42003-024-06304-4.
[19] Dubovik O, Holben B, Eck TF, Smirnov A, Kaufman YJ, King MD, et al. Variability of absorption and optical properties of key aerosol types observed in worldwide locations. J Atmos Sci 2002;59:590–608. https://doi.org/10.1175/1520-0469(2002)059. <0590:VOAAOP>2.0.CO;2.
[20] ECA, European Court of Auditors. Special report 22/2023: offshore renewable energy in the EU – Ambitious plans for growth but sustainability remains a challenge. Luxembourg: Publications Office of the European Union; 2023. https://www.eca.europa.eu/en/publications/SR-2023-22 [accessed 7 September 2024].
[21] Falchi F, Ramos F, Bará S, Sanhueza P, Jaque-Arancibia M, Damke G, Cinzano P. Light pollution indicators for all the major astronomical observatories. Mon Not R Astron Soc 2023;519(1):26–33. https://doi.org/10.1093/mnras/stac2929.
[22] Foster JJ, Smolka J, Nilsson D-E, Dacke M. How animals follow the stars. Proc R Soc B 2018;285:20172322. https://doi.org/10.1098/rspb.2017.2322.
[23] Fryc I, Bará S, Aubé M, Barentine JC, Zamorano J. On the relation between the astronomical and visual photometric systems in specifying the brightness of the night sky for Mesopically adapted observers. Leukos 2022;18(4):447–58. https://doi.org/10.1080/15502724.2021.1921593.
[24] Giles DM, Sinyuk A, Sorokin MG, Schafer JS, Smirnov A, Slutsker I, Eck TF, Holben BN, Lewis JR, Campbell JR, Welton EJ, Korkin SV, Lyapustin AI. Advancements in the Aerosol Robotic Network (AERONET) Version 3 database – automated near-real-time quality control algorithm with improved cloud screening for Sun photometer aerosol optical depth (AOD) measurements. Atmos Meas Tech 2019;12:169–209. https://doi.org/10.5194/amt-12-169-2019. 2019.
[25] Goodman JW. Introduction to fourier optics. 2nd ed. New York: McGraw-Hill; 1996. p. 134.
[26] Green RF, Luginbuhl CB, Wainscoat RJ, Duriscoe D. The growing threat of light pollution to ground-based observatories. Astron Astrophys Rev 2022;30(1). https://doi.org/10.1007/s00159-021-00138-3.
[27] Greve EL. Single stimulus and multiple stimulus threshold. Vis Res 1972;12(9):1533–43. https://doi.org/10.1016/0042-6989(72)90178-2.
[28] Guirao A, Porter J, Williams DR, Cox IG. Calculated impact of higher-order monochromatic aberrations on retinal image quality in a population of human eyes. J Opt Soc Am A 2002;19:620–8.
[29] Hess M, Koepke P, Schult I. Optical properties of aerosols and clouds: the software package OPAC. Bull Am Meteorol Soc 1998;79(5):831–44.
[30] Hüppop O, Dierschke J, Exo K-M, Fredrich E, Hill R. Bird migration studies and potential collision risk with offshore wind turbines. Ibis 2006;148:90–109. https://doi.org/10.1111/j.1474-919X.2006.00536.x.
[31] Hurtado JP, Fernandez J, Parrondo JL, Blanco E. Spanish method of visual impact evaluation in wind farms. Renew Sustain Energy Rev 2004;8(5):483–91. https://doi.org/10.1016/j.rser.2003.12.009.
[32] International Civil Aviation Organization (ICAO). Annex 14, Aerodromes. Aerodrome Design and Operations, 1. 8th ed. Montréal, Quebec, Canada : International Civil Aviation Organization; 2018. p. 197–210.
[33] Kasten F, Young AT. Revised optical air mass tables and approximation formula. Appl Opt 1989;28(22):4735–8. https://doi.org/10.1364/AO.28.004735.
[34] Kerlinger P, Gehring JL, Erickson WP, Curry R, Jain A, Guarnaccia J. Night migrant fatalities and obstruction lighting at wind turbines in North America. Wilson J Ornithol 2010;122(4):744–54. https://doi.org/10.1676/06-075.1.
[35] Kocifaj M. Light-pollution model for cloudy and cloudless night skies with ground-based light sources. Appl Opt 2007;46:3013–22. https://doi.org/10.1364/AO.46.003013.
[36] Kokologos D, Tsitoura I, Kouloumpis V, Tsoutsos T. Visual impact assessment method for wind parks: a case study in Crete. Land Use Pol 2014;39:110–20. https://doi.org/10.1016/j.landusepol.2014.03.014.
[37] Kunz TH, Arnett EB, Erickson WP, Hoar AR, Johnson GD, Larkin RP, Strickland MD, Thresher RW, Tuttle MD. Ecological impacts of wind energy development on bats: questions, research needs, and hypotheses. Front Ecol Environ 2007;5:315–24. https://doi.org/10.1890/1540-9295(2007)5 [315:EIOWED]2.0.CO;2.
[38] Land M, Nilsson DE. Animal Eyes. 2nd. Oxford: Oxford University Press; 2012.
[39] Landau AN, Fries P. Attention Samples Stimuli Rhythmically. Curr Biol 2012;22:1000–4. https://doi.org/10.1016/j.cub.2012.03.054.
[40] Lazar R, Degen J, Fiechter AS, Monticelli A, Spitschan M. Regulation of pupil size in natural vision across the human lifespan. R Soc Open Sci 2024;11:191613. https://doi.org/10.1098/rsos.191613.
[41] Leroux C, Barré K, Valet N, Kerbiriou C. Le Viol I. Distribution of common pipistrelle (Pipistrellus pipistrellus) activity is altered by airflow disruption generated by wind turbines. PLoS ONE 2024;19(5):e0303368. https://doi.org/10.1371/journal.pone.0303368.
[42] Leung DYC, Yang Y. Wind energy development and its environmental impact: review. Renew Sustain Energy Rev 2012;16(1):1031–9. https://doi.org/10.1016/j.rser.2011.09.024.
[43] Liang J, Grimm B, Goelz S, Bille J. Objective measurement of wave aberrations of the human eye with the use of a Hartmann-Shack wave-front sensor. J Opt Soc Am A 1994;11:1949–57.
[44] Liang J. Williams DR aberrations and retinal image quality of the normal human eye. J Opt Soc Am A 1997;14(11):2873–83.
[45] Lloret J, Wawrzynkowski P, Dominguez-Carrió C, Sardá R, Molins C, Gili JM, Sabatés A, Vila-Subirós J, Garcia L, Solé J, Berdalet E, Turiel A, Olivares A. Floating offshore wind farms in Mediterranean marine protected areas: a cautionary tale. ICES J Mar Sci 2023:fsad131. https://doi.org/10.1093/icesjms/fsad131.
[46] Longcore T. A compendium of photopigment peak sensitivities and visual spectral response curves of terrestrial wildlife to guide design of outdoor nighttime lighting. Basic Appl Ecol 2023;73:40–50. https://doi.org/10.1016/j.baae.2023.09.002.
[47] Losada MA, Navarro R. Point spread function of the human eye obtained by a dual double-pass method. Pure Appl Opt 1998;7:L7–13.
[48] Lothian A. Scenic perceptions of the visual effects of wind farms on South Australian landscapes. Geogr Res 2008;46:196–207. https://doi.org/10.1111/j.1745-5871.2008.00510.x.
[49] Marín C, Jafari J. StarLight: a common heritage. canary islands, spain: starlight initiative la palma biosphere reserve, instituto de astrofísica de canarias, government of the canary islands, Spanish ministry of the environment. UNESCO-MaB; 2008.
[50] Marques AT, Batalha H, Rodrigues S, Costa H, Ramos-Pereira MJ, Fonseca C, Mascarenhas M, Bernardino J. Understanding bird collisions at wind farms: an updated review on the causes and possible mitigation strategies. Biol Conserv 2014;179:40–52. https://doi.org/10.1016/j.biocon.2014.08.017.
[51] Masana E, Carrasco JM, Bará S, Ribas SJ. A multi-band map of the natural night sky brightness including Gaia and Hipparcos integrated starlight. Mon Notices Royal Astron Soc 2021;501:5443–56. https://doi.org/10.1093/mnras/staa4005.
[52] Masana E, Bará S, Carrasco JM, Ribas SJ. An enhanced version of the Gaia map of the brightness of the natural sky. Int J Sustain Light 2022;24(1):1–12. https://doi.org/10.26607/ijsl.v24i1.119.
[53] Navarro R, Losada MA. Aberrations and relative efficiency of light pencils in the living human eye. Optom Vis Sci 1997;74:540–7.
[54] Navarro R, Losada MA. Shape of stars and optical quality of the human eye. J Opt Soc Am A 1997;14:353–9.
[55] Navarro R, Moreno E, Dorronsoro C. Monochromatic aberrations and point-spread functions of the human eye across the visual field. J Opt Soc Am A 1998;15:2522–9.
[56] Natural sounds and night skies division. NPSUS National Parks Service; 2021. https://www.nps.gov/orgs/1050/index.htm [Accessed 26 September 2023].
[57] Pogson N. Magnitude of 36 of the minor planets. Mon Not R Astron Soc 1856;17(1):12–5. https://doi.org/10.1093/mnras/17.1.12.
[58] Pohl J, Hübner G, Mohs A. Acceptance and stress effects of aircraft obstruction markings of wind turbines. Energy Policy 2012;50. https://doi.org/10.1016/j.enpol.2012.07.062. 592e600.
[59] Pohl J, Rudolph D, Lyhne I, Clausen NE, Aaen SB, Hübner G, Kørnøv L, Kirkegaard JK. Annoyance of residents induced by wind turbine obstruction lights: a cross-country comparison of impact factors. Energy Policy 2021;156:112437. https://doi.org/10.1016/j.enpol.2021.112437.
[60] Porter J, Guirao A, Cox IG, Williams DR. Monochromatic aberrations of the human eye in a large population. J Opt Soc Am A 2001;18:1793–803.
[61] Rich C, Longcore T. Ecological consequences of artificial night lighting. Washington, D.C.: Island Press; 2006. p. 1.
[62] Rodrigues L., Bach L., Dubourg-Savage M.J., Karapandža B., Rnjak D., Kervyn T., Dekker J., Kepel A., Bach P., Collins J., Harbusch C., Park K., Micevski B., Minderman J. Guidelines for consideration of bats in wind farm projects – Revision 2014. EUROBATS Publication Series No. 6, Bonn, Germany: EUROBATS Secretariat; 2015. EUROBATS_6_wind turbines_engl_web_neu.pdf [Accessed 26 September 2023].
[63] Rudolph D, Kirkegaard J, Lyhne I, Clausen NE, Kørnøv L. Spoiled darkness? Sense of place and annoyance over obstruction lights from the world's largest wind turbine test centre in Denmark. Energy Res Social Sci 2017;25. https://doi.org/10.1016/j.erss.2016.12.024. 80e90.
[64] Saidur R, Rahim NA, Islam MR, Solangi KH. Environmental impact of wind energy. Renew Sustain Energy Rev 2011;15(5). https://doi.org/10.1016/j.rser.2011.02.024. 2423e2430.
[65] Schaefer BE. Astronomy and the limits of vision. Vistas Astron 1993;36:311–61. https://doi.org/10.1016/0083-6656(93)90113-X.
[66] Smallwood KS. Comparing bird and bat fatality-rate estimates among North American wind-energy projects. Wildl Soc Bull 2013;37:19–33. https://doi.org/10.1002/wsb.260.
[67] Sotillo A, le Viol I, Barré K, Bas Y, Kerbiriou C. Context-dependent effects of wind turbines on bats in rural landscapes. Biol Conserv 2024;295:110647. https://doi.org/10.1016/j.biocon.2024.110647.
[68] Teillet PM. Rayleigh optical depth comparisons from various sources. Appl Opt 1990;29:1897–900. https://doi.org/10.1364/AO.29.001897.

[69] Thibos LN, Hong X, Bradley A, Cheng X. Statistical variation of aberration structure and image quality in a normal population of healthy eyes. J Opt Soc Am A 2002;19 (12):2329–48.
[70] Thibos LN, Bradley A, Hong X. A statistical model of the aberration structure of normal, well-corrected eyes. Ophthal Physiol Opt 2002;22:427–33.
[71] van den Berg T.J.T.P., Franssen L., Coppens J.E. Ocular Media Clarity and Straylight. In Darlene A. Dartt (ed), Encyclopedia of the eye, Vol 3. Oxford, UK: Academic Press; 2010, p. 173–83.
[72] van den Berg TJTP, Franssen L, Kruijt B, Coppens JE. History of ocular straylight measurement: a review. Z fur Med Phys 2013;23:6–20. https://doi.org/10.1016/j.zemedi.2012.10.009.
[73] Voigt CC, Kaiser K, Look S, Scharnweber K, Scholz C. Wind turbines without curtailment produce large numbers of bat fatalities throughout their lifetime: a call against ignorance and neglect. Glob Ecol Conserv 2022;37:e02149. https://doi.org/10.1016/j.gecco.2022.e02149.

Environment International 82 (2015) 1–9

Contents lists available at ScienceDirect

Environment International

journal homepage: www.elsevier.com/locate/envint

# The effect of wind turbine noise on sleep and quality of life: A systematic review and meta-analysis of observational studies

Igho J. Onakpoya [a,*], Jack O'Sullivan [b], Matthew J. Thompson [c], Carl J. Heneghan [a]

[a] University of Oxford, Centre for Evidence-Based Medicine, Nuffield Department of Primary Care Health Sciences, New Radcliffe House, Radcliffe Observatory Quarter, Oxford OX2 6GG, United Kingdom
[b] Department of Health Sciences and Medicine, Bond University, Gold Coast, Queensland 4229, Australia
[c] Department of Family Medicine, University of Washington, Seattle, WA 98195-4696, USA

ARTICLE INFO

*Article history:*
Received 16 September 2014
Received in revised form 27 April 2015
Accepted 30 April 2015
Available online xxxx

*Keywords:*
Wind turbines
Annoyance
Sleep
Quality of life
Systematic review
meta-analysis

ABSTRACT

Noise generated by wind turbines has been reported to affect sleep and quality of life (QOL), but the relationship is unclear. Our objective was to explore the association between wind turbine noise, sleep disturbance and quality of life, using data from published observational studies. We searched Medline, Embase, Global Health and Google Scholar databases. No language restrictions were imposed. Hand searches of bibliography of retrieved full texts were also conducted. The reporting quality of included studies was assessed using the STROBE guidelines. Two reviewers independently determined the eligibility of studies, assessed the quality of included studies, and extracted the data. We included eight studies with a total of 2433 participants. All studies were cross-sectional, and the overall reporting quality was moderate. Meta-analysis of six studies ($n = 2364$) revealed that the odds of being annoyed is significantly increased by wind turbine noise (OR: 4.08; 95% CI: 2.37 to 7.04; $p < 0.00001$). The odds of sleep disturbance was also significantly increased with greater exposure to wind turbine noise (OR: 2.94; 95% CI: 1.98 to 4.37; $p < 0.00001$). Four studies reported that wind turbine noise significantly interfered with QOL. Further, visual perception of wind turbine generators was associated with greater frequency of reported negative health effects. In conclusion, there is some evidence that exposure to wind turbine noise is associated with increased odds of annoyance and sleep problems. Individual attitudes could influence the type of response to noise from wind turbines. Experimental and observational studies investigating the relationship between wind turbine noise and health are warranted.



## 1. Introduction

The last few decades have seen governments attempting to decrease greenhouse gas emissions (Olander et al., 2012). This response – to changes in the earth's temperature – has seen the rise of wind power (Leithead, 2007). This alternative energy source, generated by wind turbines, is one tool being employed to generate cleaner energy.

Wind turbine generators (WTGs) are devices that convert wind power into kinetic energy, and are regarded as one of the most important renewable sources of power (Leithead, 2007). Energy generated from WTGs can be used to produce electricity and drive machinery (Caduff et al., 2012; Chang Chien et al., 2011; Li and Chen, 2008). It is thought that large scale utilization of these devices can improve global climate by extracting energy from the atmosphere and altering the pattern of gaseous flow in the earth's atmosphere (Keith et al., 2004).

More recently, exposure to noise from WTGs has been reported to have negative effects on human health (Jeffery et al., 2013). People living near WTGs have reportedly experienced sleep disturbances and a reduction in the quality of life; it has been suggested that a combination of turbine noise, infrasound (sounds with frequency <20 Hz) and ground currents (stray current from electrical equipment which passes through the earth) could be responsible for these symptoms (Havas and Colling, 2011). Cases of litigation because of the unwanted health effects allegedly caused by the noise from WTGs have been reported both in the UK (Daily Mail, 2011) and the US (Oregon Herald, 2013). Very recently, the UK parliament passed a bill restricting the number, height and location of WTGs in England (UK House of Commons Library, 2015).

Studies investigating the effects of wind turbines on sleep and quality of life in individuals living in their proximity have been conducted. While the findings from a pooled meta-analyses of three studies suggested a relationship between exposure to WTG noise and annoyance (Janssen et al., 2011), a more recent review concluded that there was no evidence of a consistent relationship between WTG noise and adverse health effects (Merlin et al., 2013). Therefore, the objective of this systematic review was to explore the association between wind turbine noise, annoyance, sleep and quality of life, and also explore

*Abbreviations:* WTG, wind turbine generator; ESS, Epworth Sleepiness Scale; PSQI, Pittsburgh Sleep Quality Index.

* Corresponding author.
*E-mail address:* igho.onakpoya@phc.ox.ac.uk (I.J. Onakpoya).

http://dx.doi.org/10.1016/j.envint.2015.04.014
0160-4120/

the influence of other moderating factors on these outcomes, using data from published observational studies.

## 2. Methods

We conducted electronic searches in the following databases: Medline, Embase and Global health. Each database was searched from inception till June 2014. MeSH terms used included wind turbine, wind energy, clean energy, annoyance, sleep, and quality of life (a MEDLINE search strategy is included as a web Appendix 1). We also searched Google Scholar for relevant conference proceedings, and hand searched the bibliography of retrieved full texts. An updated search of the databases was conducted on November 28, 2014. Case–control, cross-sectional, and cohort studies were considered for inclusion. To be included in the review, studies had to report annoyance, sleep or quality of life as outcomes in subjects living in proximity with wind turbines. Studies not comparing participants based on the proximity of their homes to WTGs were excluded. No age, language or time restrictions were imposed. Where necessary, contact with study investigators was made to request additional data.

The reporting quality of included studies was evaluated using a checklist adapted from the STROBE (Strengthening of Reporting of Observational Studies in Epidemiology) guidelines (von Elm et al., 2007). Data was systematically extracted by two reviewers [IJO and JOS] using a piloted spreadsheet of pertinent variables including baseline demographics, study location, distances of homes from wind turbines, SPLs, assessment of exposure and outcome. These were independently cross-checked by two other reviewers [MJT and CJH]. Disagreements were resolved through consensus. Our main outcomes were annoyance, sleep disturbance and quality of life (QOL). We also examined the influence of other background noise, visual perception and socio-economic factors on reported outcomes.

Odds ratios (ORs) were used to measure associations between wind turbine noise and annoyance or sleep disturbance. Using the random-effects model of the software for meta-analyses (Review Manager, Version 5.3 (2011)), we calculated the ORs and 95% confidence intervals (CI) for the studies which had sufficient data for statistical pooling. We used sound pressure level (SPL) reference ranges of <40 dB for lower exposure and >40 dB for higher exposure to wind turbine noise in the analyses; these limits correspond to the World Health Organisation (WHO) guideline recommendations for indoor community noise levels suitable for night-time sleep (Berglund et al., 1999). Where SPLs were not available, we used the reported near ("near group") and far ("far group") distances from WTGs for high and low SPLs respectively. Subgroup analyses by SPLs or distances from WTGs were used to test the robustness of overall analyses. Sensitivity analyses by meta-analysing studies with larger sample sizes or with higher respondent rates (≥50%) were used to investigate heterogeneity using the $I^2$ statistic; values of 25%, 50%, and 75% indicated low, medium, and high statistical heterogeneity respectively. Where statistical combination of reported data was considered inappropriate, such data was reported narratively.

### 2.1. Definitions

For the purpose of this review, annoyance was defined as a constellation of psychosocial and/or psychological symptoms — "feelings of being bothered, exasperation at being interrupted by noise, and symptoms such as headache, fatigue and irritability" (Anonymous, 1977). Sleep disturbance was defined as any interruption of an individual's normal sleep–wake pattern (Cormier, 1990). A change in an individual's quality of life was measured based on their own perceptions, with regard to their own goals, expectations, standards and concerns (WHO, 1997).

## 3. Results

Our electronic searches returned 148 non-duplicate citations, out of which 18 potentially eligible articles were identified (Fig. 1). One article (Ambrose et al., 2012) was excluded because the study was conducted in only one residential apartment and another two (Maffei et al., 2013; Van Renterghem et al., 2013) because they were virtual experimental studies conducted in subjects not residing within the vicinity of WTGs. Two articles (Verheijen et al., 2011; Pedersen and Larsman, 2008) were excluded because they were modelling studies, the latter of which used results from two studies already included in the review. One article was excluded because it explored the effects of road traffic noise using data from a study included in the review (Pedersen et al., 2010) and another two because they did not distinguish subjects by distance from WTGs or SPLs (Harry, 2007; Morris, 2012). Two articles (Nissenbaum et al., 2011; Pedersen et al., 2009) were excluded because more complete versions of their reports were included in the review. Thus eight studies (Bakker et al., 2012; Krogh et al., 2011; Magari et al., 2014; Nissenbaum et al., 2012; Pawlaczyk-Łuszczyńska et al., 2014; Pedersen and Persson Waye, 2004, 2007; Shepherd et al., 2011) with a total of 2433 participants were included in the review. The key details of the studies are shown in Tables 1, 2a and 2b.

All included studies were of cross-sectional design (Table 1). Seven studies reported appropriate recruitment and sampling strategies, and all used objective and validated measures to compute outcome variables. The studies also used appropriate statistical methods to compare groups, but only half (50%) adequately reported sample size calculations. All studies reported adequate statistical analysis, and baseline demographics for participants in the high and low exposure groups were generally similar. The response rate for questionnaires ranged from 37% to 93%.

Annoyance was measured on a 5-point scale (ranging from did not notice to very annoyed) using questionnaires that enquired about attitudes towards wind turbines; one study (Pawlaczyk-Łuszczyńska et al., 2014) used a 6-point scale that included "extremely annoyed" variable after "very annoyed". In all the studies, annoyance from exposure to WTG noise implied being rather annoyed, very annoyed or extremely annoyed. Sleep disturbance (defined in the studies as interruption of normal sleep patterns) was assessed from the general questionnaire administered in seven studies (Bakker et al., 2012; Krogh et al., 2011; Magari et al., 2014; Pawlaczyk-Łuszczyńska et al., 2014; Pedersen and Persson Waye, 2004, 2007; Shepherd et al., 2011), and measured by Pittsburgh Sleep Quality Index (PSQI) in the eighth (Nissenbaum et al., 2012) — this same study assessed daytime sleepiness using the Epworth Sleepiness Scale (ESS). Quality of life was measured in three studies by general health questionnaire (GHQ) (Bakker et al., 2012; Pawlaczyk-Łuszczyńska et al., 2014), short form 36 (SF-36v2) (Nissenbaum et al., 2012), and health-related quality of life (HRQOL) (Shepherd et al., 2011). Two studies used unspecified masked questionnaires that addressed health and general well-being (Pedersen and Persson Waye, 2004, 2007); these questionnaires were described as validated. One study (Krogh et al., 2011) did not use a validated questionnaire to assess quality of life and another (Magari et al., 2014) did not report quality of life as an outcome.

The study locations ranged from rural to semi-rural and metropolitan built-up areas (Table 2a), with varying population densities and terrain. The distance of homes from WTGs varied between 0 and 8 km, and the number of WTGs in the individual studies ranged from 16 to 1846. The emission levels for the WTGs in the studies were measured using A-weighted scales (a filtering method aimed at mimicking responses to sound by the human ear) with 8 m/s downwind, and power generated from the turbines ranged between 0.15 and 2300 kW.

The mean age of the respondents across all the studies was 46 to 58 years (Table 2b). One study (Krogh et al., 2011) did not report the socio-economic status of respondents, while another (Bakker et al.,

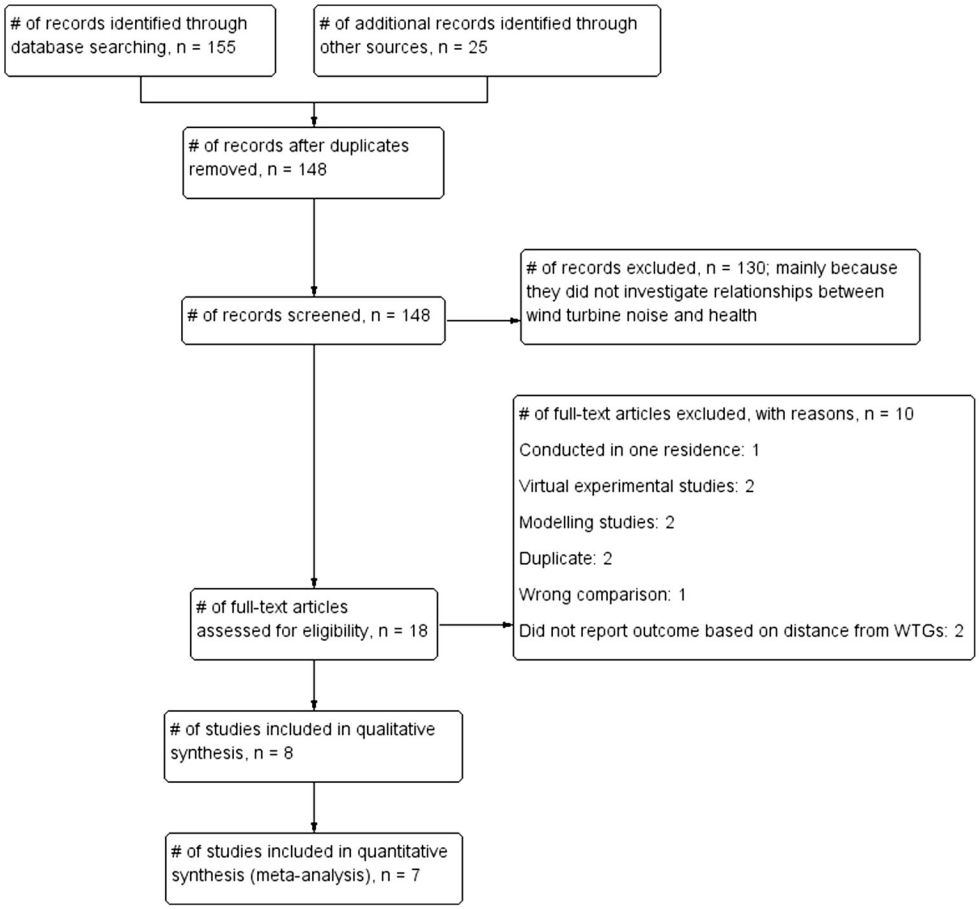


The Flow Diagram has been adapted from the online version of the PRISMA statement, 2009. Available from: http:// www.prisma-statement.org/statement.htm

**Fig. 1.** Flow diagram showing the process for inclusion of studies examining the relationship between wind turbine noise and health.

2012) reported a significantly higher proportion of respondent who received higher education in the high SPL group compared with the low SPL group ($p < 0.001$). The remaining studies did not report significant differences in the baseline demographics of respondents. All the respondents in two studies (Magari et al., 2014; Nissenbaum et al., 2012) had financial benefits from WTGs (Table 2b). Reported background noises

**Table 1**
Reporting quality of studies exploring the association between turbine noise, sleep and quality of life.

| Study ID<br>Country of study | Study design | Appropriate recruitment strategy? | Appropriate sampling technique? | Response rate | Representative sample? | Relevant outcome measures?[a] | Power calculation? | Appropriate statistical analysis? | Evidence of bias? |
|---|---|---|---|---|---|---|---|---|---|
| Bakker et al., 2012<br>The Netherlands | Cross-sectional | Yes — questionnaire sent to houses | Yes | 37% | Yes | Yes | Yes | Yes | No |
| Krogh et al., 2011<br>Canada | Cross-sectional | Yes — postal & hand-delivered questionnaire | Unclear | 88.9% | Yes | Yes | Unclear | Yes | No |
| Magari et al., 2014<br>USA | Cross-sectional | Yes — administered in person by two field personnel | Yes | 92.9% | Yes | Yes | Unclear | Yes | No |
| Nissenbaum et al., 2012<br>USA | Cross-sectional | Yes — telephone and door to door | Yes | 40% | Yes | Yes | Unclear | Yes | No |
| Pawlaczyk-Łuszczyńska et al., 2014<br>Poland | Cross-sectional | Yes — postal questionnaire | Yes | 71% | Yes | Yes | Yes | Yes | No |
| Pedersen and Persson Waye, 2004<br>Sweden | Cross-sectional | Yes — questionnaire sent to houses | Yes | 68.4% | Yes | Yes | Yes | Yes | No |
| Pedersen and Persson Waye, 2007<br>Sweden | Cross-sectional | Yes — postal questionnaire | Yes | 57.6% | Yes | Yes | Yes | Yes | No |
| Shepherd et al., 2011<br>New Zealand | Cross sectional | Yes — postal | Yes | 33% | Yes | Yes | Unclear | Yes | No |

[a] All the outcomes measured were subjective, except for Pedersen and Persson Waye (2007) which measured visual perception using visual angle of WTGs from homes.

**Table 2a**
Main characteristics of studies investigating the association between wind turbine noise, sleep and quality of life.

| Study ID | Study location & site topography | Number of participants | SPLs & distance from WTGs | Power & number of WTGs | Outcomes | Tools used to measure outcomes |
|---|---|---|---|---|---|---|
| Bakker et al. (2012) | 1. Rural area (with no major road within 500 m from the closest wind turbine) 2. Rural area with a major road within 500 m from the closest wind turbine 3. More densely populated built up area Flat terrain | 725 | 21–54 dB (average: 35 dB) 0–2.5 km | ≥500 kW (0.5 MW); 1846 | Annoyance, sleep disturbance, psychological stress | Annoyance: 5-point ordinal scale & 2 Likert scales. Sleep disturbance: Frequency |
| Krogh et al. (2011) | 5 WTG areas with anecdotal reports of adverse health effects | 109 | 0.35–2.4 km | 1.65 MW: 5 WTG project areas | Sleep disturbance | WindVOiCe Survey Questionnaire |
| Magari et al. (2014) | 1. Rural area 2. 5 receptor locations within wind turbine park; two locations outside the park as comparator | 62 | 0.4–4 km | 1.5 MW; 84 | Annoyance, health effects | Validated general questionnaire |
| Nissenbaum et al. (2012) | 2 rural areas — 'low-lying, tree-covered island.' Flat terrain | 79 | 32–57 dB 0.4–6.6 km | 1.5 MW; 31 | Sleep quality, mental health | Sleep disturbance: PSQI & ESS QOL: (SF-36v2) |
| Pawlaczyk-Łuszczyńska et al. (2014) | 1. 3 populated areas in Central & Northwest Poland 2 Flat terrain 3. Mainly agricultural, but railroads and/or roads also present | 156 | 30–50 dB 0.24–2.5 km | 0.15, 1.5 & 2 MW; total number of wind turbines 108 | Annoyance, mental health | Annoyance: 5-point ordinal scale Sleep and QOL: GHQ |
| Pedersen and Persson Waye (2004) | 5 wind turbine areas; flat terrain | 351 | <30 to >40 dB 0.15–1.2 km | 14 WTGs: 600–650 kW; 2 WTGs: 150 & 500 kW | Noise perception, annoyance, sleep disturbance | Validated general questionnaire: Annoyance: unipolar annoyance scale Sleep disturbance: presence or absence |
| Pedersen and Persson Waye (2007) | 7 wind turbine areas; different landscapes in terrain and urbanisation (flat and 'complex'–rocky or altitude); suburban and rural | 754 | 31.4–38.2 dB (mean: 33.4). 0.6–1 km (mean: 0.78 km) | >500 kW; 478 | Perception, annoyance, sleep quality, quality of life | Validated general questionnaire Annoyance: unipolar annoyance scale Sleep disturbance: presence or absence |
| Shepherd et al. (2011) | 2 semi-rural coastal areas differentiated by their proximity to wind turbines; hilly terrain | 197 | 20–50 dB <2 to 8 km | 2300 kW; 66 | Annoyance, sleep disturbance, quality of life (health) | Questionnaire with subcomponents: Annoyance: 7-item scale Sleep: 7-item scale QOL: HRQOL |

Abbreviations: SPLs: sound pressure levels; WTGs: wind turbine generators; dB: decibels; km: kilometres; kW: kilowatts; MW: megawatts; PSQI: Pittsburgh Sleep Quality Index; ESS: Epworth Sleepiness Scale; QOL: quality of life; GHQ: general health questionnaire; HRQOL: health-related quality of life.

included road traffic noise, noises from birds and household pets, and other machinery.

One study (Pedersen and Persson Waye, 2004) was funded by a grant from a research foundation, while four (Bakker et al., 2012; Magari et al., 2014; Pawlaczyk-Łuszczyńska et al., 2014; Pedersen and Persson Waye, 2007) were funded by government grants. The authors in two studies (Nissenbaum et al., 2012; Shepherd et al., 2011) failed to declare their sources of funding. The authors in all studies were affiliated with public institutions, except in two studies (Magari et al., 2014; Nissenbaum et al., 2012) where authors were affiliated to public health consultancy firms. One study (Krogh et al., 2011) was not funded by any entity.

### 3.1. Relationship between wind turbine noise and annoyance

Two studies (Krogh et al., 2011; Nissenbaum et al., 2012) did not report annoyance as an outcome. Meta-analysis of the remaining six studies ($n = 2364$; Fig. 2) revealed a significant increase in the odds of being rather annoyed, annoyed or very annoyed by wind turbine noise (OR: 4.08; 95% CI: 2.37 to 7.04; $I^2 = 63\%$; $p < 0.00001$). Subgroup analyses by SPLs or distance from WTG did not change the direction of the results (Fig. 2). Sensitivity analysis of three studies with larger sample sizes ($n = 1793$) revealed that the odds of being annoyed by wind turbine noise is significantly increased with higher SPLs (OR: 6.94; 95% CI: 4.36 to 11.03; $I^2 = 10\%$; $p < 0.00001$). Meta-analysis of four studies with higher respondent rates ($n = 1313$) revealed that the odds of being annoyed by living close to wind turbines is statistically significant (OR: 3.00; 95% CI: 1.87 to 4.80; $I^2 = 0\%$; $p < 0.00001$).

### 3.2. Relationship between wind turbine noise and sleep disturbance

Two studies (Nissenbaum et al., 2012; Shepherd et al., 2011) did not provide suitable data for statistical pooling. One of these (Nissenbaum et al., 2012) reported the "near group" as having significantly worse sleep scores for both PSQI ($p = 0.046$) and ESS ($p = 0.03$); and two subjects in the "near group" were diagnosed with insomnia compared to none in the "far group". In the second study (Shepherd et al., 2011), participants with greater exposure to WTG noise reported significantly worse sleep scores ($p = 0.0006$). For the remaining six studies which provided suitable data, three (Bakker et al., 2012; Pedersen and Persson Waye, 2004, 2007) used low SPL values of <30 dB as controls, while two (Krogh et al., 2011; Magari et al., 2014) compared groups based on the distances of respondents' from WTGs. Meta-analysis revealed a significant increase in the odds of reporting sleep disturbances with greater exposure to noise from WTGs (OR 2.94; 95% CI: 1.98 to 4.37; $I^2 = 0\%$; $p < 0.00001$; Fig. 3). Subgroup analysis by SPLs or distance did not result in a change in the direction of the results. A similar result was observed when five studies with higher respondents' rates ($n = 810$) were meta-analysed (OR: 2.76; 95% CI: 1.65 to 4.62; $I^2 = 0\%$; $p = 0.0001$). Sensitivity analyses of studies with larger sample sizes

**Table 2b**
Demographic characteristics of respondents and influence of moderating factors in the included studies.

| Study ID | Mean age | Average duration at home | Socio-economic status | Background noises and their influence on outcome | Visual perception of WTGs and influence on outcome | Financial relationship with WTG and influence on outcome |
|---|---|---|---|---|---|---|
| Bakker et al. (2012) | 51 years | Not reported; economic benefits had no statistically significant impact on perception of the sound. | Proportion of respondents with higher education was significantly higher with those living in high SPLs ($p < 0.001$) | Road traffic; aircraft; railways; industry & shunt yards<br>Exposure to WTG sound did not lead to noise annoyance amongst respondents who lived in areas classified as noisy and reported that they could hear the sound. Sound exposure predicted noise annoyance ($r = 0.54$) amongst respondents who reported that they could hear WTG sound and lived in areas classified as quiet | 73% of respondents in rural areas and 54% in built-up areas could see at least one WTG from their dwellings<br>The probability of being annoyed by WTG sound was higher if they were visible ($p < 0.001$) | Of 100 persons who benefitted from WTG, 76 were in high SPL group.<br>The proportion of benefiting respondents who were rather or very annoyed by WTG sound was 4 times lower compared to the non-benefiters (12 versus 3%; $p < 0.05$), despite the fact that respondents who benefited economically were exposed to higher levels of WTG sound and noticed the WTG sound more often |
| Krogh et al. (2011) | 52 years | Not reported | Not reported | Not reported | Not reported | Not reported |
| Magari et al. (2014) | 51 years | 18 years | Similar for residents | Amongst participants annoyed by WTG noise, 60% were affected daily or a few times weekly by noise, 92% by television or radio interference, and 54% by shadows or reflections<br>None of the indoor or outdoor SPL measurements significantly correlated with other environmental factors — noise, pollution, and landscape littering | On average 19 WTGs were visible<br>General annoyance was significantly correlated with opinion of altered landscape due to WTG ($p < 0.0001$) | All residents benefitted from WTG: substantial property tax reduction; free trash removal<br>Respondents who directly benefitted from WTGs were not less annoyed than other respondents. 90% of participants were satisfied or very satisfied with their environment |
| Nissenbaum et al. (2012) | 57.5 years | 14 to 21 years in near group<br>24 to 30 years in far group | No significant differences | Not reported | WTGs were visible to a majority of respondents<br>The visual impact of WTG on those living closest to turbines was greater compared with those living further away | All residents benefit financially: reduced electricity costs and/or increased tax revenues<br>Fear of reducing property value led to downplaying of adverse health effects |
| Pawlaczyk-Łuszczyńska et al. (2014) | 46 years | Not reported | Comparable between groups | Mainly agricultural terrain with low traffic intensity railways, roads.<br>Did not analyse the impact of terrain and urbanisation on annoyance related to WTG noise. There was high positive correlation between as well as between the respondents' sensitivity to noise and sensitivity to landscape littering ($p < 0.0000001$) | 97% of respondents could see 1 or more WTGs from their dwelling, backyard or garden.<br>There was high positive correlation between general attitude towards WTGs and attitude to their visual impact ($p < 0.0000001$) | 2.6% benefitted from WTG: type of benefit unspecified |
| Pedersen and Persson Waye (2004) | 48 years | Not reported | No statistically significant differences between groups | Road traffic, rail traffic, neighbours. No significant differences in variables related to noise sensitivity, attitude, or health between the different sound categories<br>At lower sound categories, no respondents were disturbed in their sleep by WTG noise, but 16% of the 128 respondents living at SPLs >35 dB reported sleep disturbance due to WTG noise | WTGs were visible from "many" directions.<br>Respondents' attitude to the visual impact of WTGs on the landscape scenery influenced noise annoyance ($p < 0.001$).<br>No impact of visual perception on sleep disturbance | 95% did not own or share a WTG |
| Pedersen and Persson Waye (2007) | 51 years | 14 to 16 years in near group<br>15 to 16 years in far group | Similar for residents | The rural dwellers were the respondents' group with the highest proportion of noise sensitivity (56–59%)<br>There was a significant increase in the odds of annoyance from WTGs in rural areas (quiet) compared with suburban areas (noisy), OR 1.8. [1.25 to 2.51] | The highest proportion of respondents who could see at least 1 WTG was rural (88–91%)<br>Perception of annoyance correlated with SPLs ($p < 0.001$)<br>Both the objective variable "vertical visual angle" and the subjective report of visibility of wind turbines increased the odds of being annoyed: 1.2 | Not reported |

(continued on next page)

**Table 2b** (*continued*)

| Study ID | Mean age | Average duration at home | Socio-economic status | Background noises and their influence on outcome | Visual perception of WTGs and influence on outcome | Financial relationship with WTG and influence on outcome |
|---|---|---|---|---|---|---|
| | | | | | (95% CI: 1.03 to 1.42), and 10.9 (95% CI: 1.46 to 81.92) respectively | |
| Shepherd et al. (2011) | Range: 18–71 years | Not reported | Matched between groups | No differences between groups for traffic ($p = 0.154$) or neighbourhood ($p = 0.144$) noise annoyance | Not reported specifically due to masking of the study intent | Not reported |

($n = 838$) revealed a significant increase in the odds of sleep disturbances with higher SPLs (OR: 3.24; 95% CI: 2.03 to 5.18; $I^2 = 0\%$; $p < 0.00001$).

Another study (Pedersen and Persson Waye, 2004) reported no statistically significant correlations between sleep quality and sensitivity to WTG noise. One study (Pawlaczyk-Łuszczyńska et al., 2014) reported a significant relationship between the frequency of annoyance and sleep disturbance ($p < 0.05$).

### 3.3. Relationship between wind turbine noise and quality of life (QOL)

Because of discrepancies in the methods used to assess QOL across studies, a meta-analysis was not considered appropriate. One study (Bakker et al., 2012) reported significant correlations between wind turbine noise and psychological distress in quiet ($p < 0.05$), and both noisy and quiet areas ($p < 0.01$). Another (Nissenbaum et al., 2012) reported that participants in the high noise exposure group had significantly lower QOL (lower GHQ scores) compared with the low exposure group ($p = 0.002$), and a third (Pawlaczyk-Łuszczyńska et al., 2014) reported a weak but significant correlation between wind turbine noise and mental health based on the responses on the GHQ ($p < 0.00625$) — in the same study, a significantly greater proportion of respondents in the "near group" reported that WTG noise has impacted negatively on their health ($p < 0.05$). Another study (Pedersen and Persson Waye, 2007) reported that SPLs were not correlated with general wellbeing of study participants, but annoyed respondents felt significantly more tired ($p = 0.05$) and tense ($p < 0.05$) in the mornings. In one study (Shepherd et al., 2011), the high SPL group had lower HRQOL and environmental QOL scores compared with the lower SPL group ($p = 0.017$ and 0.018 respectively).

One study (Krogh et al., 2011) reported a significant relationship between proximity related WTG noise and excessive tiredness ($p = 0.03$) (the residents in the groups closer to the WTGs reported a higher percentage of excessive tiredness). This same study showed a trend towards increased risk of headache with closer proximity to WTGs ($p = 0.1$). Another study (Nissenbaum et al., 2012) reported a near significant increase in the proportion of respondents receiving new psychotropic prescriptions (after WTG installation) in the "near group" compared with the "far group" (24% vs 0.07 $p = 0.06$). While 90% of participants in one study (Magari et al., 2014) reported being either satisfied or being very satisfied with their environment, the "near group" respondents in another study (Shepherd et al., 2011) were significantly less satisfied compared with the "far group" ($p = 0.03$).

### 3.4. Influence of background noise and settings on outcomes

In two studies (Bakker et al., 2012; Pedersen and Persson Waye, 2007), episodes of annoyance at a given WTG noise level were significantly higher in quiet areas compared with areas classified as noisy. A third study (Pedersen and Persson Waye, 2004) reported no significant

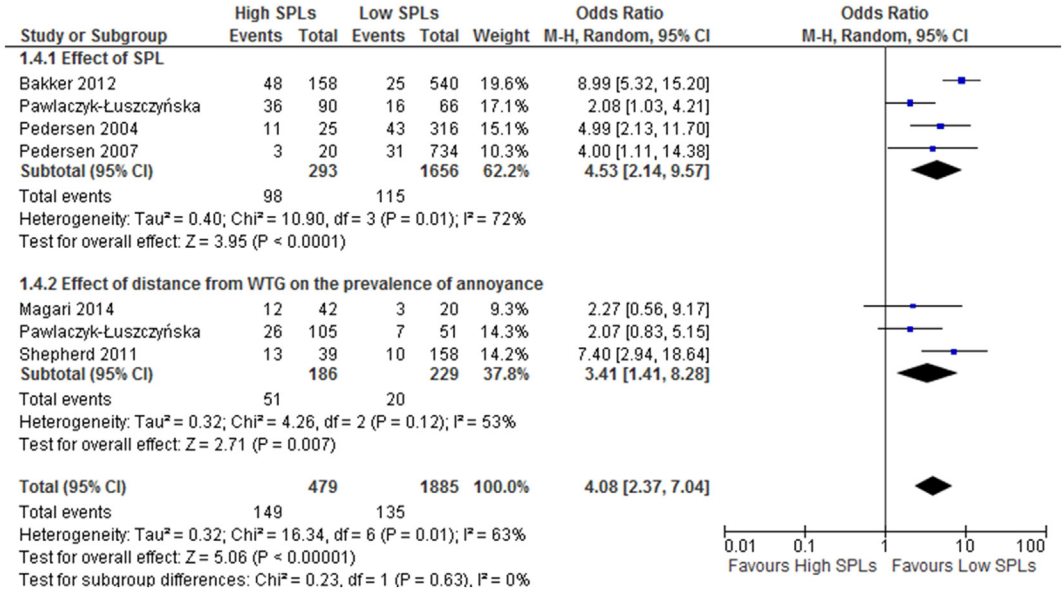


*Annoyance variable includes "rather annoyed", "annoyed" or "very annoyed". For Magari 2014 and Shepherd 2011, near distances ("high SPLs") are defined as homes located within 2km from the nearest wind turbine generator (WTG); far distances ("low SPLs") were homes located at least 2km from the nearest WTG. For Pawlaczyk-Łuszczyńska 2014, these corresponded to <800m and >800m respectively.

**Fig. 2.** Relationship between wind turbine noise and annoyance.* *Annoyance variable includes "rather annoyed", "annoyed" or "very annoyed". For Magari et al. (2014) and Shepherd et al. (2011), near distances ("high SPLS") are defined as homes located within 2 km from the nearest wind turbine generator (WTG); far distances ("low SPLS") were homes located at least 2 km from the nearest WTG. For Pawlaczyk-Łuszczyńska et al. (2014), these corresponded to <800 m and >800 m respectively.

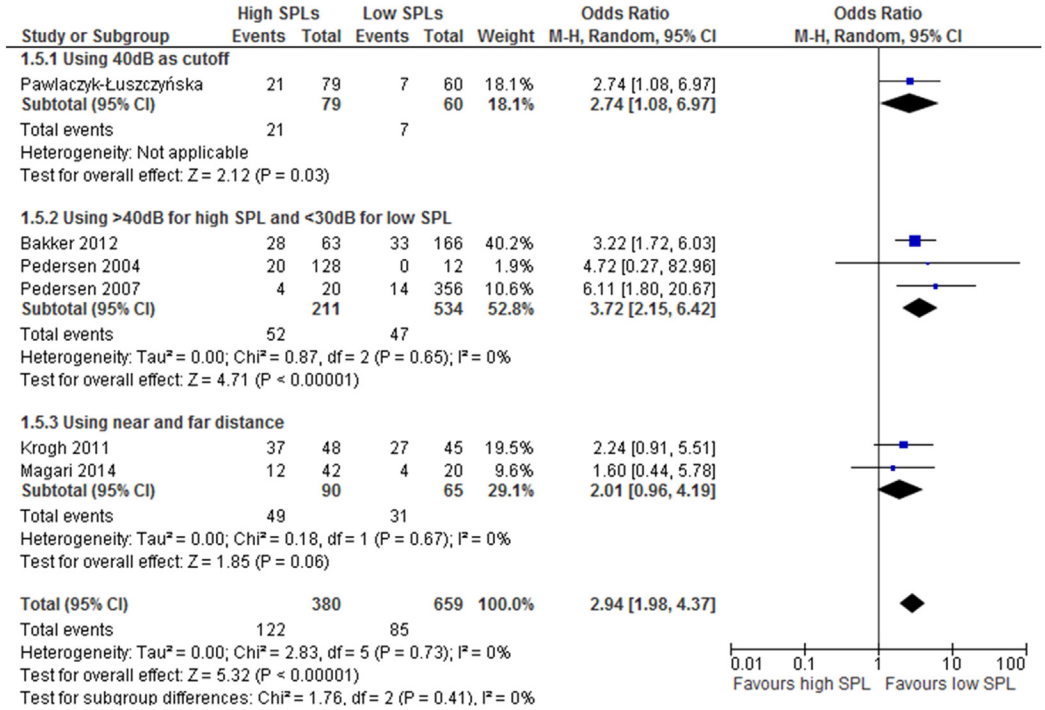


*For Magari 2014, near distances ("high SPLs") are defined as homes located within 2km from the nearest WTG; for Krogh 2011, near distances ("high SPLs") were homes located within 700m of the nearest WTG.

**Fig. 3.** Relationship between wind turbine noise and sleep.* *For Magari et al. (2014), near distances ("high SPLS") are defined as homes located within 2 km from the nearest WTG; for Krogh et al. (2011), near distances ("high SPLS") were homes located within 700 m of the nearest WTG.

difference between groups for different sound categories; however, there was a trend towards increased sleep disturbances with higher SPLs. A fourth study (Shepherd et al., 2011) reported no differences between groups for traffic ($p = 0.15$) or neighbourhood ($p = 0.14$) noise annoyance (Table 2b). One study (Pawlaczyk-Łuszczyńska et al., 2014) did not analyse the impact of other environmental noise on outcomes.

### 3.5. Effect of visual perception on outcomes

Six studies reported data on the relationship between visual perception of WTG and its influence on outcomes (Table 2b). Five of these (Bakker et al., 2012; Magari et al., 2014; Pawlaczyk-Łuszczyńska et al., 2014; Pedersen and Persson Waye, 2004, 2007) reported a significant positive correlation between visual perception of WTGs and the episodes of annoyance; one of these studies (Pedersen and Persson Waye, 2007) also reported a significant correlation when an objective variable (visual angle) was used to explore the relationship. The sixth study (Nissenbaum et al., 2012) reported that visual impact of WTG on those living closest to turbines was greater compared with those living further away, but did not report whether this was significant. The authors of one study (Shepherd et al., 2011) did not explore the effect of visual perception on outcomes because they wanted to mask the study intent.

### 3.6. Influence of economic benefit from WTG on outcome

The influence of economic benefit on outcome was inconsistent across the three studies that explored the relationship. One study (Bakker et al., 2012) reported a significantly lower rate of annoyance amongst respondents who benefitted economically from WTGs compared with respondents who had no benefit ($p < 0.001$), while another study (Magari et al., 2014) reported no significant difference in outcomes between groups. Respondents in the third study (Nissenbaum et al., 2012) indicated that the fear of reducing property value led to downplaying of adverse health effects. Two studies (Pawlaczyk-Łuszczyńska et al., 2014; Pedersen and Persson Waye, 2004) in which ≤5% of participants had financial benefits from WTGs did not report whether financial incentives resulted in differences in outcome rates.

## 4. Discussion

Our results provide evidence that living in areas with WTGs appears to result in "annoyance", and may also be associated with sleep disturbances and decreased quality of life. The results of included studies also suggest that visual perception of WTGs is correlated with increased episodes of annoyance, and the reported adverse effects from WTGs are more prominent in quiet areas compared with noisy ones. The results of our meta-analysis corroborate the findings of a previous meta-analysis of three studies which reported that wind turbine noise is significantly associated with annoyance (Janssen et al., 2011). However, our pooled data contained twice as many studies compared with that report. Our results contradict the findings of another review that concluded that there was no consistent relationship between WTG noise and adverse health effect (Merlin et al., 2013). In contrast to that report, we statistically combined data, and we included evidence from two new studies that were not available for that review. The results of our meta-analysis also support the findings of a more recent systematic review which concluded that exposure to WTG noise increases the risk of annoyance and self-reported sleep disturbance (Schmidt and Klokker, 2014). In comparison with that report, we meta-analysed study data, and also included one study which was not available in that report. Our meta-analyses results should be interpreted with caution due to the variation in outcome measures, and moderate heterogeneity observed in some of the analyses.

The results of our meta-analysis suggest that exposure to WTG noise can elicit annoyance. However, the moderate to large heterogeneity observed in the subgroup analysis limits the firmness of any conclusions that can be drawn from the meta-analytic results. Some authors have

suggested that the perception of rhythmic sound pressure by the inner ear could result in negative health outcomes (Enbom and Enbom, 2013; Gohlke et al., 2008; Todd et al., 2008), but this has been refuted by others (Knopper and Ollson, 2011). In addition, other investigators have concluded that it is impossible to distinguish between noises generated by WTGs from that caused by wind itself (Bilski, 2012). Until better tools to assess the impact of WTGs are developed, the relationship between WTG noise and annoyance will remain controversial.

Our meta-analytic results indicate that living close to WTGs increases the odds of experiencing sleep disturbances. Results of studies which did not provide adequate data for statistical pooling were also consistent with this finding. The evidence from the included studies also suggests that sleep disturbance is positively correlated with annoyance and this supports the findings from research conducted in other types of settings (Aasvang et al., 2007; van den Berg et al., 2014; Lee et al., 2011).

We observed a relationship between noise generated from WTGs and reduction in QOL in a majority of the included studies, and this corroborates with previous research reports (Basner et al., 2014; Stansfeld and Matheson, 2003). Pathways showing inter-relationships between annoyance, sleep disturbance and QOL have been modelled (Bakker et al., 2012). However, sleep disturbance has also been shown to independently correlate with a poorer QOL (Lee et al., 2009), and the results of the studies included in our review showed a trend towards a reduction in QOL with increased frequency of sleep disturbances.

It appears that background noise from other environmental sources may influence attitude towards WTGs. The evidence from the studies in our review suggests that the reported adverse effects were more prominent in quiet areas compared with noisy ones. However, residents in quiet areas had a greater proportion of individuals with noise sensitivity and this attitude could have played a role in their responses. Because A-weighted scales (used by most WTGs) totally ignore sound frequencies below 20 Hz, the use of G-weighted scales (specifically designed for infrasound) for measurement of WTG noise has been suggested (Farboud et al., 2013); however, the G-weighted scale has been demonstrated to fluctuate significantly at low frequencies (Bilski, 2012). Other authors have reported that noise from WTGs are too low to cause any harm at distances over 305 m (Knopper and Ollson, 2011; O'Neal et al., 2011). A universally agreed method for measuring sound emissions from WTGs will help clarify these uncertainties.

The results of our review indicate that visual interference could determine attitudes to WTG. There was a greater likelihood of annoyance or less satisfaction if respondents could either see WTGs from their residence, or if they thought WTGs distorted their landscape. This finding supports the conclusions of other authors who reported that visual interference from WTGs may actually be responsible for the annoyance, rather than the noise generated by the wind turbines (Jeffery et al., 2014). Based on this finding, we are less certain if the noise from WTGs themselves actually results in the annoyance, sleep disturbances or reduced quality of life observed in our systematic review and meta-analysis; this issue warrants further investigation.

It is unclear to what extent economic ties with WTGs influenced participants' responses. The inconsistency in the relationship reported across studies makes it difficult to ascertain whether benefitting financially from WTGs affects attitude. Therefore, we are unable to draw conclusions about this relationship based on present evidence.

## 5. Strengths and limitations

The strengths of this systematic review and meta-analysis are the use of a robust search strategy to identify relevant studies, and our success with obtaining additional data through contact with investigators of studies that we included in the review. The overall quality of the evidence from the included studies was moderate. In addition, heterogeneity was reduced in most of our sensitivity and subgroup analyses, and the results of these analyses were also consistent with overall analyses. However, we recognize some limitations. The small number of included studies prevented us from performing a funnel plot to test for publication bias. It could be argued that publication bias may have occurred in either direction, given the different financial and social implications of WTG and their placement. It is also possible that participants' responses could have been biased; especially in settings where anecdotal reports of adverse effects from WTGs have been documented (Krogh et al., 2011; Magari et al., 2014; Nissenbaum et al., 2012), or in situations where administered questionnaires did not mask the topic of interest (Bakker et al., 2012; Pawlaczyk-Łuszczyńska et al., 2014; Pedersen and Persson Waye, 2004, 2007). It is difficult to gauge the extent to which residual background noise or financial benefits influenced the responses received from study participants. The variations in topography, design, number and power of WTGs, and variation in outcome measures limit the conclusions that could be drawn from our analyses. Finally, apart from one study (Pedersen and Persson Waye, 2007) which used an objective method (visual angle) to assess the relationship between visual perception and annoyance, the response variables measured in the included studies are all subjective and do not establish causality for the relationships examined.

### 5.1. Implications for research and policy

Independently funded studies exploring the relationships of wind turbines on human health are warranted; in particular, objective outcome measures that separate auditory and visual effects of WTGs should be developed. Experimental and observational studies investigating the relationship between noise exposure at WTGs and health effects should be conducted. Such studies should also explore whether benefitting economically from WTGs influences attitudes. In addition, research aimed at determining the minimum distance of homes from wind turbines at which there will be no risk of interference with health is advocated.

Further, greater monitoring of the sound emission levels from WTGs, especially those located in quiet rural communities, is advocated. A balance between individual and community preferences should be struck when making decisions about where to site WTGs. This will help to ensure the maximisation of the climatic, provider and consumer benefits from future constructions of WTGs.

## 6. Conclusion

The evidence from cross-sectional studies suggests that exposure to wind turbine noise may be associated with increased frequency of annoyance and sleep problems. Evidence also suggests that living in proximity to WTGs could be associated with changes in the quality of life. Individual attitudes could influence the type of response to noise from WTGs.

## Authors' contribution

IJO and JOS were involved with protocol design, data extraction, data-analysis and interpretation, and co-drafting of the manuscript. MJT was involved with data-analysis and interpretation, and co-drafting of the manuscript. CJH was involved with protocol design, data analysis and interpretation, and co-drafting of the manuscript.

## Funding

None.

## Competing interest

Professor Heneghan has received payment for running educational courses at the University of Oxford and for external teaching and training. He also receives royalties for books (Evidence Based Toolkit series by Blackwell BMJ Books). Dr Onakpoya, Dr O'Sullivan and Prof. Thompson have no interests to disclose.

## Acknowledgement

We would like to thank James Shepherd, Carmen Krogh and Shannon Magari for providing additional information and clarification on their studies.

## Appendix A. Supplementary data

Supplementary data to this article can be found online at http://dx.doi.org/10.1016/j.envint.2015.04.014.

## References

Aasvang, G.M., Engdahl, B., Rothschild, K., 2007. Annoyance and self-reported sleep disturbances due to structurally radiated noise from railway tunnels. Appl. Acoust. 68 (9), 970–981 (September).

Ambrose, S.E., Rand, R.W., Krogh, C.E., 2012. Wind turbine acoustic investigation: infrasound and low-frequency noise—a case study. Bull. Sci. Technol. Soc. http://dx.doi.org/10.1177/0270467612455734.

Anonymous, 1977. Noise, annoyance, and mental health. Lancet 1 (8021), 1090–1091 (May 21).

Bakker, R.H., Pedersen, E., van den Berg, G.P., Stewart, R.E., Lok, W., Bouma, J., 2012. Impact of wind turbine sound on annoyance, self-reported sleep disturbance and psychological distress. Sci. Total Environ. 425, 42–51 (May 15).

Basner, M., Babisch, W., Davis, A., Brink, M., Clark, C., Janssen, S., Stansfeld, S., 2014. Auditory and non-auditory effects of noise on health. Lancet 383 (9925), 1325–1332 (Apr 12).

Berglund, B., Lindvall, T., Schwela, D.H., 1999. Guidelines for community noise. Available at:. http://www.bvsde.paho.org/bvsci/i/fulltext/noise/noise.pdf.

Bilski, B., 2012. Factors influencing social perception of investments in the wind power industry with an analysis of influence of the most significant environmental factor — exposure to noise. Pol. J. Environ. Stud. 21 (2), 289–295.

Caduff, M., Huijbregts, M.A., Althaus, H.J., Koehler, A., Hellweg, S., 2012. Wind power electricity: the bigger the turbine, the greener the electricity? Environ. Sci. Technol. 46 (9), 4725–4733. http://dx.doi.org/10.1021/es204108n (May 1, Epub 2012 Apr 20).

Chang Chien, J.R., Tseng, K.C., Yan, B.Y., 2011. Design of a hybrid battery charger system fed by a wind-turbine and photovoltaic power generators. Rev. Sci. Instrum. 82 (3), 035107 (Mar).

Cormier, R.E., 1990. Sleep disturbances. Chapter 77. In: Walker, K., Dallas, W., Hurst, J.W. (Eds.), Clinical Methods: The History, Physical, and Laboratory Examinations, 3rd edition Buttersworth, Boston.

Enbom, H., Enbom, I.M., 2013. Infrasound from wind turbines—an overlooked health hazard. Lakartidningen 110 (32–33), 1388–1389 (Aug 7–20).

Farboud, A., Crunkhorn, R., Trinidade, A., 2013. 'Wind turbine syndrome': fact or fiction? J. Laryngol. Otol. 127, 222–226.

Gohlke, J.M., Hrynkow, S.H., Portier, C.J., 2008. Health, economy, and environment: sustainable energy choices for a nation. Environ. Health Perspect. 116 (6), A236–A237 (Jun).

Harry, A., 2007. Wind turbines, noise and health. February, http://docs.wind-watch.org/wtnoise_health_2007_a_harry.pdf (Accessed 20th November, 2014).

Havas, M., Colling, D., 2011. Wind turbines make waves: why some residents near wind turbines become ill. Bull. Sci. Technol. Soc. 31 (5), 414–426.

Oregon Herald, 2013. Man files $5 million lawsuit for noisy wind turbines. 11th August, Available at:. http://www.oregonherald.com/oregon/local.cfm?id=4327.

Janssen, S.A., Vos, H., Eisses, A.R., Pedersen, E., 2011. A comparison between exposure–response relationships for wind turbine annoyance and annoyance due to other noise sources. J. Acoust. Soc. Am. 130 (6), 3746–3753 (Dec).

Jeffery, R.D., Krogh, C., Horner, B., 2013. Adverse health effects of industrial wind turbines. Can. Fam. Physician 59 (5), 473–475 (May).

Jeffery, R.D., Krogh, C.M., Horner, B., 2014. Industrial wind turbines and adverse health effects. Can. J. Rural Med. 19 (1), 21–26 (Winter).

Keith, D.W., Decarolis, J.F., Denkenberger, D.C., Lenschow, D.H., Malyshev, S.L., Pacala, S., Rasch, P.J., 2004. The influence of large-scale wind power on global climate. Proc. Natl. Acad. Sci. U. S. A. 101 (46), 16115–16120 (Nov 16).

Knopper, L.D., Ollson, C.A., 2011. Health effects and wind turbines: a review of the literature. Environ. Health 10, 78. http://dx.doi.org/10.1186/1476-069X-10-78 (Sep 14).

Krogh, C.M.E., Gillis, L., Kouwen, N., Aramini, J., 2011. WindVOiCe, a self-reporting survey: adverse health effects, industrial wind turbines, and the need for vigilance monitoring. Bull. Sci. Technol. Soc. 31, 334.

Lee, M., Choh, A.C., Demerath, E.W., Knutson, K.L., Duren, D.L., Sherwood, R.J., Sun, S.S., Chumlea, W.M., Towne, B., Siervogel, R.M., Czerwinski, S.A., 2009. Sleep disturbance in relation to health-related quality of life in adults: the Fels Longitudinal Study. J. Nutr. Health Aging 13 (6), 576–583 (Jun).

Lee, S., Kim, K., Choi, W., Lee, S., 2011. Annoyance caused by amplitude modulation of wind turbine noise. Noise Control Eng. J. 59, 38–46.

Leithead, W.E., 2007. Wind energy. Philos. Transact. A Math. Phys. Eng. Sci. 365 (1853), 957–970 (Apr 15).

Li, H., Chen, Z., 2008. Overview of different wind generator systems and their comparisons. IET Renew. Power Gener. 2 (2), 123–138.

Maffei, L., Iachini, T., Masullo, M., Aletta, F., Sorrentino, F., Senese, V.P., Ruotolo, F., 2013. The effects of vision-related aspects on noise perception of wind turbines in quiet areas. Int. J. Environ. Res. Public Health 10 (5), 1681–1697. http://dx.doi.org/10.3390/ijerph10051681 (Apr 26).

Magari, S.R., Smith, C.E., Schiff, M., Rohr, A.C., 2014. Evaluation of community response to wind turbine-related noise in western New York state. Noise Health 16 (71), 228–239 (Jul-Aug).

Merlin, T., Newton, S., Ellery, B., Milverton, J., Farah, C., 2013. Systematic Review of the Human Health Effects of Wind Farms. National Health and Medical Research Council, Canberra.

Morris, M., 2012. 'Waterloo Wind Farm Survey', electronic self-published report. http://www.wind-watch.org/news/wp-content/uploads/2012/07/Waterloo-Wind-Farm-Survey-April-2012-Select-Committee.pdf (Accessed 29th November, 2014).

Nissenbaum, M., Aramini, J., Hanning, C., 2011. Adverse health effects of industrial wind turbines: a preliminary report. Presented at: 10th International Congress on Noise as a Public Health Problem (ICBEN) 2011, London, UK.

Nissenbaum, M.A., Aramini, J.J., Hanning, C.D., 2012. Effects of industrial wind turbine noise on sleep and health. Noise Health 14 (60), 237–243 (Sep-Oct).

Olander, L.P., Cooley, D.M., Galik, C.S., 2012. The potential role for management of U.S. public lands in greenhouse gas mitigation and climate policy. Environ. Manag. 49 (3), 523–533. http://dx.doi.org/10.1007/s00267-011-9806-1 (Mar).

O'Neal, R.D., Hellweg Jr., R.D., Lampeter, R.M., 2011. Low frequency noise and infrasound from wind turbines. Noise Control Eng. J. 59, 135–157.

Pawlaczyk-Łuszczyńska, M., Dudarewicz, A., Zaborowski, K., Zamojska-Daniszewska, M., Waszkowska, M., 2014. Evaluation of annoyance from the wind turbine noise: a pilot study. Int. J. Occup. Med. Environ. Health 27 (3), 364–388 (Jun).

Pedersen, E., Larsman, P., 2008. The impact of visual factors on noise annoyance among people living in the vicinity of wind turbines. J. Environ. Psychol. 28, 379–389.

Pedersen, E., Persson, Waye K., 2004. Perception and annoyance due to wind turbine noise—a dose–response relationship. J. Acoust. Soc. Am. 116 (6), 3460–3470 (Dec).

Pedersen, E., Persson, Waye K., 2007. Wind turbine noise, annoyance and self-reported health and well-being in different living environments. Occup. Environ. Med. 64 (7), 480–486 (Jul).

Pedersen, E., van den Berg, F., Bakker, R., Bouma, J., 2009. Response to noise from modern wind farms in The Netherlands. J. Acoust. Soc. Am. 126 (2), 634–643 (Aug).

Pedersen, E., van den Berg, F., Bakker, R., Bouma, J., 2010. Can road traffic mask sound from wind turbines? Response to wind turbine sound at different levels of road traffic sound. Energy Policy 38, 2520–2527.

Review Manager (RevMan), 2011. [Computer Program]. Version 5.3. The Nordic Cochrane Centre, The Cochrane Collaboration, Copenhagen.

Schmidt, J.H., Klokker, M., 2014. Health effects related to wind turbine noise exposure: a systematic review. PLoS One 9 (12), e114183 (Dec 4).

Shepherd, D., McBride, D., Welch, D., Dirks, K.N., Hill, E.M., 2011. Evaluating the impact of wind turbine noise on health-related quality of life. Noise Health 13 (54), 333–339 (Sep-Oct).

Stansfeld, S.A., Matheson, M.P., 2003. Noise pollution: non-auditory effects on health. Br. Med. Bull. 68, 243–257.

The Daily Mail UK, 2011. Couple driven out of home by constant hum of wind farm launch landmark battle to get a peaceful night's sleep. 5th July, Available at:, http://www.dailymail.co.uk/news/article-2011162/Wind-farms-whoom-whoom-whoom-noise-drove-mad-farmers-claiming-3m-tell-High-Court.html (Accessed 10th May, 2014).

Todd, N.P., Rosengren, S.M., Colebatch, J.G., 2008. Tuning and sensitivity of the human vestibular system to low-frequency vibration. Neurosci. Lett. 444 (1), 36–41.

UK House of Commons Library, 2015. Planning for onshore wind farms — Commons Library Standard Note. Available at:, http://www.parliament.uk/business/publications/research/briefing-papers/SN04370/planning-for-onshore-wind-farms (Accessed 10th May, 2014).

van den Berg, F., Verhagen, C., Uitenbroek, D., 2014. The relation between scores on noise annoyance and noise disturbed sleep in a public health survey. Int. J. Environ. Res. Public Health 11 (2), 2314–2327 (Feb 21).

Van Renterghem, T., Bockstael, A., De Weirt, V., Botteldooren, D., 2013. Annoyance, detection and recognition of wind turbine noise. Sci. Total Environ. 456–457, 333–345. http://dx.doi.org/10.1016/j.scitotenv.2013.03.095 (Jul 1).

Verheijen, E., Jabben, J., Schreurs, E., Smith, K.B., 2011. Impact of wind turbine noise in The Netherlands. Noise Health 13 (55), 459–463. http://dx.doi.org/10.4103/1463-1741.90331 (Nov-Dec).

von Elm, E., Altman, D.G., Egger, M., Pocock, S.J., Gøtzsche, P.C., et al., 2007. Strengthening the Reporting of Observational Studies in Epidemiology (STROBE) statement: guidelines for reporting observational studies. PLoS Med. 4 (10), e296. http://dx.doi.org/10.1371/journal.pmed.0040296.

World Health Organization, 1997. Programme on mental health. WHOQOL: measuring quality of life. http://www.who.int/mental_health/media/68.pdf (Accessed 20th May, 2014).

PHILOSOPHICAL TRANSACTIONS A

rsta.royalsocietypublishing.org

Research

**Cite this article:** Van Renterghem T. 2017 Sound propagation from a ridge wind turbine across a valley. *Phil. Trans. R. Soc. A* **375**: 20160105.
http://dx.doi.org/10.1098/rsta.2016.0105

Received: 17 June 2016
Accepted: 29 September 2016

One contribution of 11 to a theme issue 'Wind energy in complex terrains'.

**Subject Areas:**
computational physics, atmospheric science, environmental engineering, acoustics

**Keywords:**
outdoor sound propagation, wind turbine, undulating terrain, parabolic equation method

**Author for correspondence:**
Timothy Van Renterghem
e-mail: timothy.vanrenterghem@ugent.be

# Sound propagation from a ridge wind turbine across a valley

Timothy Van Renterghem

Department of Information Technology, Ghent University, iGent tower, Technologiepark 15, 9052 Zwijnaarde, Belgium

TVR, 0000-0003-0435-5485

Sound propagation outdoors can be strongly affected by ground topography. The existence of hills and valleys between a source and receiver can lead to the shielding or focusing of sound waves. Such effects can result in significant variations in received sound levels. In addition, wind speed and air temperature gradients in the atmospheric boundary layer also play an important role. All of the foregoing factors can become especially important for the case of wind turbines located on a ridge overlooking a valley. Ridges are often selected for wind turbines in order to increase their energy capture potential through the wind speed-up effects often experienced in such locations. In this paper, a hybrid calculation method is presented to model such a case, relying on an analytical solution for sound diffraction around an impedance cylinder and the conformal mapping (CM) Green's function parabolic equation (GFPE) technique. The various aspects of the model have been successfully validated against alternative prediction methods. Example calculations with this hybrid analytical–CM–GFPE model show the complex sound pressure level distribution across the valley and the effect of valley ground type. The proposed method has the potential to include the effect of refraction through the inclusion of complex wind and temperature fields, although this aspect has been highly simplified in the current simulations.

This article is part of the themed issue 'Wind energy in complex terrains'.

## 1. Introduction

In order to fulfil the renewable energy targets that have been set in many countries, the number of wind turbines

THE ROYAL SOCIETY PUBLISHING

is expected to increase significantly in the near future. Among the different environmental impacts associated with wind turbines (such as landscape and visual impact, shadow flicker, impact on wildlife, electromagnetic interference and climate change [1]), noise issues remain the key environmental factor controlling the extent of a wind farm's development [2]. Even at low A-weighted sound pressure levels, there is a substantial negative perception towards wind turbine noise [3–8]. Therefore, noise impact assessments are commonly required during the planning phase.

Positioning wind turbines on ridges can potentially intensify momentum extraction from the wind flow [9], caused by the so-called wind speed-up effect [10–12]. Parameters of relevance include hill shape, the terrain upwind of the hill, atmospheric stability and whether or not the hill is forested [9–12].

However, there is little research, to the author's knowledge, regarding sound propagation from a ridge-mounted wind turbine to receptor locations across an adjacent valley, although the measurement-based studies of Evans & Cooper [13] have highlighted the importance of topography, including valleys, for wind turbine noise propagation. Established knowledge from other types of environmental noise sources cannot be easily transferred to the present case due to the unique positioning of the source high above a ridge. Physical phenomena that could be relevant to the present case include amplification of sound due to the valley (potentially mediated or intensified by the valley shape and its acoustic ground impedance), partial shielding by the ridge, and atmospheric refraction and turbulent scattering of sound waves due to the complex flow fields that are expected in such a geometry. Both the hilly topography and the presence of a turbine will add to the complexity of the flow. In this work, some of these aspects are studied by means of numerical sound propagation modelling.

Study of the foregoing expected sound propagation effects demands an advanced outdoor sound propagation technique. However, consideration additionally needs to be given to the computational cost, and therefore also the practical applicability of any such advanced techniques. Meta-analysis of (perception) studies with regard to wind turbine noise annoyance [14] state that, below 35 dBA, negative effects are generally not found. Logically, the latter defines the distance of concern. For large horizontal-axis wind turbines, with total source power levels easily exceeding 100 dBA when operating near their maximum power production, a propagation distance of minimum 1 km from the source should be attained. Knowing that wind turbine noise emission spectra typically show a maximum near the octave band of 1 kHz [15,16], and given that sufficiently detailed wave propagation techniques need sub-wavelength discretization, the numerical problem becomes challenging regarding spatio-temporal discretization.

An interesting candidate is the parabolic equation (PE) method (see e.g. [17,18]). The simplification to one-way sound propagation allows efficient solving of the governing sound propagation equations. In addition, a refracting atmosphere can be accounted for in detail. For many cases involving long-distance sound propagation, reasonably accurate predictions can be made with this methodology. Of specific interest is the Green's function parabolic equation (GFPE) method [19,20], as this allows forward stepping at multiples of the wavelength, in contrast to the sub-wavelength step spacing of most other advanced techniques.

The GFPE, however, cannot be readily used to model sound propagation from a ridge-mounted wind turbine. The inclusion of undulating terrain will be discussed in this work, and a number of specific problems will be dealt with. Focus is on accurately accounting for the effect of terrain undulation in the case of a source positioned high above a ridge. In addition, some example calculations are provided to show the potential of the proposed model.

In this paper, the specific wind and temperature fields near a ridge wind turbine are not considered. Only a highly simplified approach is used to model downwind sound propagation, although more complex flow fields could be rather easily included in the GFPE methodology. Turbulence scattering and coherence loss are also not considered in this work. Note that, although there is strong progress in computational fluid dynamics modelling, providing detailed flow fields in the case of a ridge-mounted wind turbine still remains highly challenging.

## 2. The Green's function parabolic equation method in undulating terrain

### (a) Basic stepping equation

The two-dimensional stepping equation of the GFPE method is summarized by equation (2.1). Some basic features of this technique are discussed below, but a detailed derivation and analysis can be found elsewhere [17,19,20]. In this forward propagation approach, the vertical array of pressures $p$ at range $r + \mathrm{d}r$ is extrapolated from the previous column at range $r$. Thus

$$p(r+\mathrm{d}r,z) = \exp(-\mathrm{i}\mathrm{d}r k_0)\overbrace{\exp(\mathrm{i}\mathrm{d}r(k-k_0))}^{\text{refraction term}} \times \overbrace{\left\{\frac{1}{2\pi}\int_{-\infty}^{\infty}\exp\left(\mathrm{i}\mathrm{d}r\sqrt{k_0^2-k_z^2}\right)\exp(\mathrm{i}k_z z)\,\mathrm{d}k_z\int_0^{\infty}\exp(-\mathrm{i}k_z z')p(r,z')\,\mathrm{d}z'\right.}^{\text{direct wave}} + \overbrace{\frac{1}{2\pi}\int_{-\infty}^{\infty}R(k_z)\exp\left(\mathrm{i}\mathrm{d}r\sqrt{k_0^2-k_z^2}\right)\exp(\mathrm{i}k_z z)\,\mathrm{d}k_z\int_0^{\infty}\exp(\mathrm{i}k_z z')p(r,z')\,\mathrm{d}z'}^{\text{ground-reflected wave}} + \overbrace{\left.2\mathrm{i}\frac{k_0}{Z}\exp\left(-\mathrm{i}\frac{k_0}{Z}z\right)\exp\left(\mathrm{i}\mathrm{d}r\sqrt{k_0^2-(k_0/Z)^2}\right)\int_0^{\infty}\exp\left(-\mathrm{i}\frac{k_0}{Z}z'\right)p(r,z')\,\mathrm{d}z'\right\}}^{\text{surface wave}}, \quad (2.1)$$

with i the imaginary unit, $(r, z)$ the position in, respectively, the horizontal and vertical direction with $\mathrm{d}r$ and $\mathrm{d}z$ their spatial discretization steps, $Z$ the ground impedance normalized to that of (unbounded) air ($=\rho_0 c_0$, with $\rho_0$ the mass density of air and $c_0$ the sound speed; local reaction approximation), $k_0$ the reference wavenumber (at the ground surface), $k$ the height-dependent wavenumber ($k = 2\pi f/c$, with $f$ the sound frequency under consideration) and $k_z$ the wavenumber in the (vertical) spatial (Fourier) domain.

Some distinct contributions in equation (2.1) can be identified, namely the direct wave, the ground-reflected wave and a surface wave. Refraction can be efficiently approached by a phase correction due to wavenumber variations with height. Temperature (and to a lesser extent humidity) variations with height are directly linked to changes in sound speed [17,18] involving no approximations. The horizontal components of the wind speed (parallel to the ground) can be approached by an equivalent increase in the sound speed (i.e. the so-called 'effective sound speed' approach [17,18]). This stepwise calculation of the acoustic fields allows both the sound speed profile and the ground parameters to be made range-dependent.

The integrals appearing in the direct and ground-reflected wave terms can be efficiently calculated by relying on the Fourier transform and its inverse, for which numerically very efficient algorithms are commonly available, such as the fast Fourier transform.

In order to represent the wind turbine noise source as a point source, the calculations will rely on the equivalence between (coherent) line source propagation (i.e. the two-dimensional solution) and point source propagation (i.e. the three-dimensional solution) when expressing sound pressure levels relative to free-field sound propagation [21] (see §4).

### (b) Including terrain undulations

Various approaches for introducing undulating terrain in the PE method can be found, like the general terrain PE (GTPE) [22], the rotated reference frame approach [23–25] (GFrPE), a stair-step terrain approach using Kirchoff's method [26] and the conformal mapping (CM) method [17,27,28].

The GTPE can be seen as a generalization of the Crank–Nicolson PE (CNPE) method. This method is applicable to arbitrary terrain profiles and uses terrain-following coordinates. However, analysis has shown that the local slope angles should not exceed roughly 30° [17].

In addition, the CNPE is much less efficient than the GFPE, as stepping in the propagation direction needs sub-wavelength discretization.

The rotated reference frame approach is applicable to the GFPE. The curved ground is treated as a succession of flat zones with different slope angles. The sound field in each domain starts from an array of pressure values, orthogonal to the local slope, as calculated from the previous domain. A number of reduced propagation steps are thus needed near the interface to accurately construct the next domain's starting field, which can strongly increase computing times [25]. Sudden slope changes along the propagation path are difficult to handle.

The stair-step approach might be attractive due to its simplicity. The terrain profile is reduced to a succession of best-fitting steps that are each treated as small vertical barriers. The part of the sound field covered by each step is then set to zero. This method further needs a vertical coordinate shift to continue propagation from the top of the next step. Combining the foregoing approach with variable step widths provides great flexibility in describing terrain profiles. However, only reflection on horizontal surfaces is modelled. This means that waves reflected obliquely in the direction of sound propagation cannot subsequently interfere along the propagation path. Only part of the acoustic energy will be sent in that direction due to diffraction at step corners, thereby potentially resulting in a significant loss in accuracy.

In this study, the CM method will be used, which is a computationally highly efficient approach to account for undulating terrain. The CM method is based on the theoretically perfect analogy between a circularly curved ground surface with radius $R_c$ and a refracting atmosphere with the following exponential sound speed profile $c$:

$$c = c_0 e^{z/R_c}, \tag{2.2}$$

with $R_c > 0$ for concave ground and $R_c < 0$ for convex ground, $z$ the height above the ground and $c_0$ the reference sound speed.

The shielding caused by convex terrain can thus be approached by sound propagating over flat terrain in an upwardly refracting atmosphere, while concave ground is simulated by a downwardly refracting atmosphere. A change in sound speed profile comes at almost no additional computational cost in the PE model. Note that such artificially refracting atmospheres due to ground curvature are typically much stronger than those observed due to real wind flows in the atmospheric boundary layer. The latter, however, can be superimposed on the artificial profile due to ground curving, thus allowing account to be taken of both terrain undulation and atmospheric refraction.

The main limitation here is the need for simplification to circularly curved terrain segments. Care is needed to account for the coordinate transform between the real (curved ground) system and the artificially refractive flat PE domain.

## 3. Hybrid analytical–conformal mapping–Green's function parabolic equation model

When applying the GFPE to the specific case of sound propagation across a valley from a ridge-mounted wind turbine, two fundamental problems appear.

Firstly, a direct application of the CM approach would actually mean that the source becomes oriented perpendicular to the curved ground. Clearly, such a configuration, as schematically illustrated in figure 1*a*, deviates strongly from a typical wind turbine case. A more realistic scenario, still consistent with the CM approach, can be achieved by placing two circular ground segments in series [17,27] (figure 1*b*). The geometry of interest is thus idealized to sound propagation over a small convex circular segment representing the ridge (with artificial upward refraction), followed by sound propagation over part of a large concave cylinder representing the valley (with artificial downward refraction).

A second fundamental problem when using the PE method for such a case is that sound propagation can only be accurately described in a relative small cone, horizontally centred around

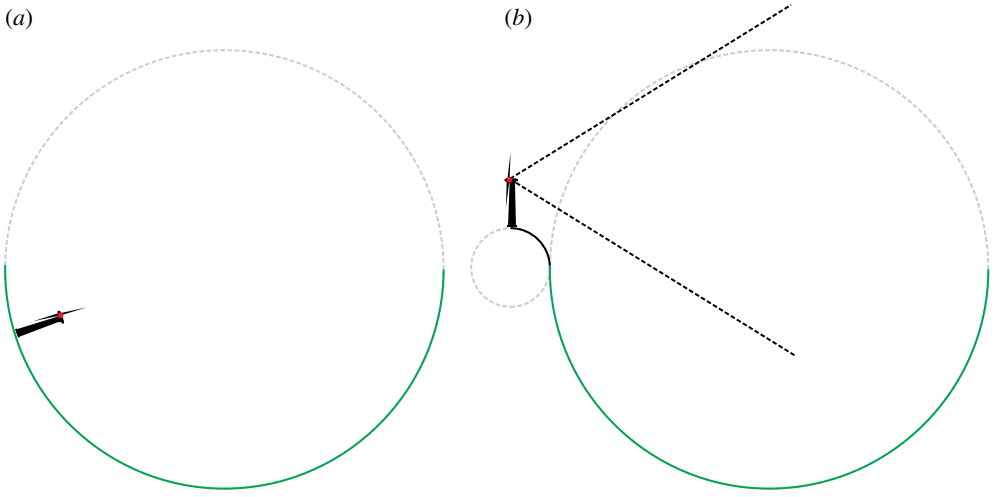


**Figure 1.** Schematics of two fundamental problems associated with CM–GFPE modelling applied to sound propagation from a ridge wind turbine. (Online version in colour.)

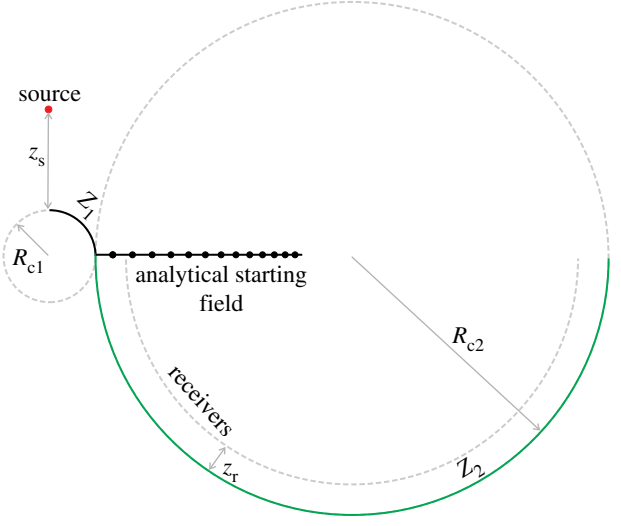


**Figure 2.** Geometry of the hybrid analytical–CM–GFPE model for simulating sound propagation from an elevated sound source, positioned at a ridge (radius $R_{c1}$, source height $z_s$), towards a valley (radius $R_{c2}$, receiver heights $z_r$). $Z_1$ and $Z_2$ are the ground impedances of the ridge and valley parts, respectively. (Online version in colour.)

the source. In the current context with a source at a large height, a major part of the valley would be artificially put in an acoustic shadow zone (figure 1*b*), leading to inaccurate results. Although applying a higher-order source approximation could extend the cone with correct predictions [17], at the source side of the valley this problem would still remain.

The solution to this problem is found in the fact that the GFPE method is able to commence from any vertical array of pressures that can be accurately calculated at sub-wavelength spacing. There are actually three possibilities. Most commonly used is a Gaussian starter [17] as the first column of pressures, representing a monopole source. Accuracy up to larger propagation angles can be achieved by a higher-order approach of the latter [17]. Secondly, another full-wave technique can be used to produce a starting field at close distance from the source [21,29]. A third

option, as done in this work, uses the analytical solution for coherent line source diffraction around an impedance cylinder (with circular cross-section), with the line source parallel to the cylinder axis (summarized in appendix A).

As a result, the current hybrid analytical–CM–GFPE model does not suffer from angle limitations in the source region. As shown in figure 2, sound propagation over exactly one-quarter of the cylinder, representing the ridge, is simulated to facilitate the coupling to the valley part. This avoids complicated interpolation at the interface with the valley section. Note that, for the valley part, the ground can be further split up in segments with different impedance. The starting field must be characterized on a vertical grid with a (logarithmically) decreasing spacing towards higher positions. This is necessary to comply with the CM coordinate transform from the curved surface to a grid with a uniform vertical spacing in an (artificially) refracting environment [17,27].

## 4. Numerical validation

The numerical codes and their parameter choices employed in this study have been validated in two-dimensional cases by intercomparison with other prediction methods (see figure 3 and table 1 for an overview). Note that, although the numerical techniques proposed for the hybrid model (see §3) are theoretically sound, such an exercise is still useful: it is stressed, e.g. in [30], that the GFPE method needs some critical parameter choices, potentially strongly impacting on numerical accuracy. All surfaces were chosen to be rigid, allowing a detailed check of the accuracy of predicted interferences, these becoming most pronounced in such a case. Sound pressure levels relative to free-field propagation (unbounded domain) are compared in all cases. This allows focus to be maintained on the physical wave aspects since geometrical divergence, which is always present, is excluded.

In case A, the axisymmetric [17] CM–GFPE is validated against the analytical solution for sound diffraction around a cylinder (see appendix A) in the case of circularly convex ground. Note that the CM–GFPE could give rise to numerical issues when source and/or receiver heights are large relative to the ground radius [17]. Therefore, a somewhat larger radius was chosen than would otherwise be appropriate for the ridge part of the model.

In case B, the axisymmetric CM–GFPE is compared with the two-dimensional finite-difference time-domain (FDTD) technique [31] for the case of a circularly concave ground segment. The FDTD technique can be considered as a reference solution over a wide range of acoustical applications. A somewhat larger radius for the ground curvature is now taken compared with validation case A, but still smaller than the radius of a typical valley. This is because the FDTD method is computationally highly demanding. Note that the effect of ground curvature on sound propagation becomes visible at a short distance (see later), thereby justifying this choice. The FDTD code as used here, in its basic form, employs a staircase approach, leading to scattering at the rigid edges of the steps. This effect can be strongly reduced when analysing a lower sound frequency, ensuring a high ratio between wavelength and spatial discretization step.

In case C, the methodology to develop the GFPE solution from an analytically constructed, coherent line source starting field is compared with the analytical solution of sound propagation over flat rigid ground, directly starting from the source. A two-ray analytical solution for a coherent line source is used for the latter [17,32,33].

Validation case A shows good agreement between the analytical solution describing sound propagating around a circular rigid cylinder and the CM–GFPE. Figure 4 shows the sound field in the transformed coordinate system used by the CM–GFPE (with $r$ the distance along the arc). Receivers are positioned at a fixed height relative to the arc. At close distance, the angle limitation of the PE method becomes visible, as discussed before. Note that an eighth-order starting field was used here (see §3 and [17]), thereby partly mitigating this inaccuracy. The CM–GFPE yields somewhat less pronounced destructive interference dips that appear at short distance in this particular case; the (very) low levels due to sound wave cancelling are typically not reached with a numerical technique. Near the constructive interferences, differences amount to 0.6 dB. In the deep shadow zone, some small oscillations in the CM–GFPE could be observed.

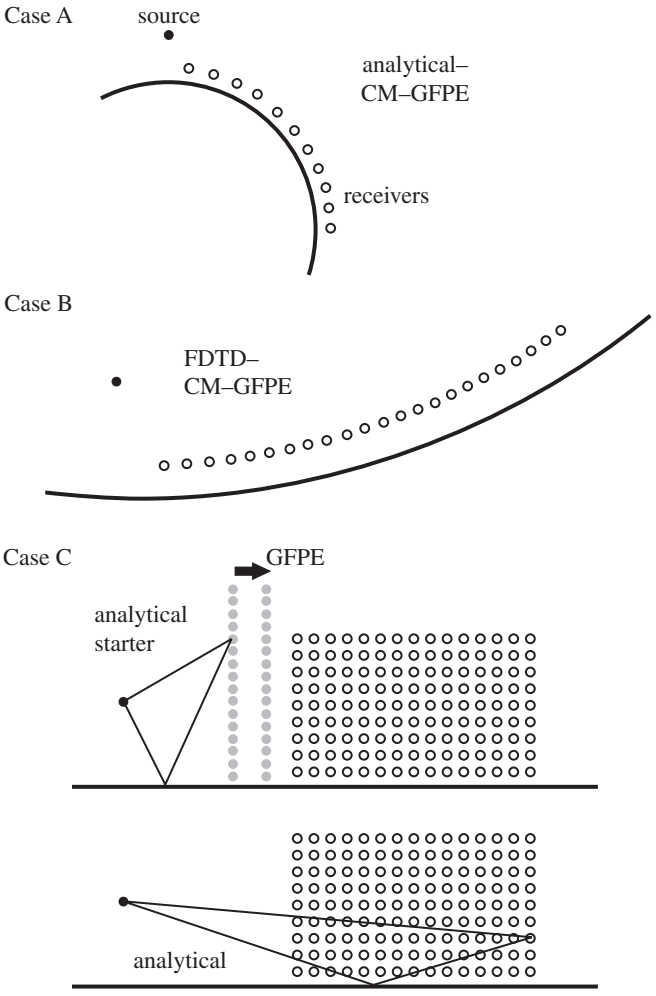


**Figure 3.** Schematics of the validation cases considered.

**Table 1.** Cross-validation cases considered, with indication of their geometries.

| parameter | case A | case B | case C |
|---|---|---|---|
| models compared | CM–GFPE versus analytical solution | CM–GFPE versus FDTD | GFPE with analytical starter versus (full) analytical solution |
| sound frequency (Hz) | 500 | 250 | 500 |
| $R_c$ (m) | −50 (convex) | 100 (concave) | $\infty$ (flat) |
| $z_s$ (m) | 5 | 5 | 5 |
| $z_r$ (m) | 1 | 2 | zone of receivers |
| maximum angle over which propagated | $\pi/2$ | $\pi/6$ | zone of receivers |
| maximum propagation distance along arc (m) | 78 | 50 | 550 |

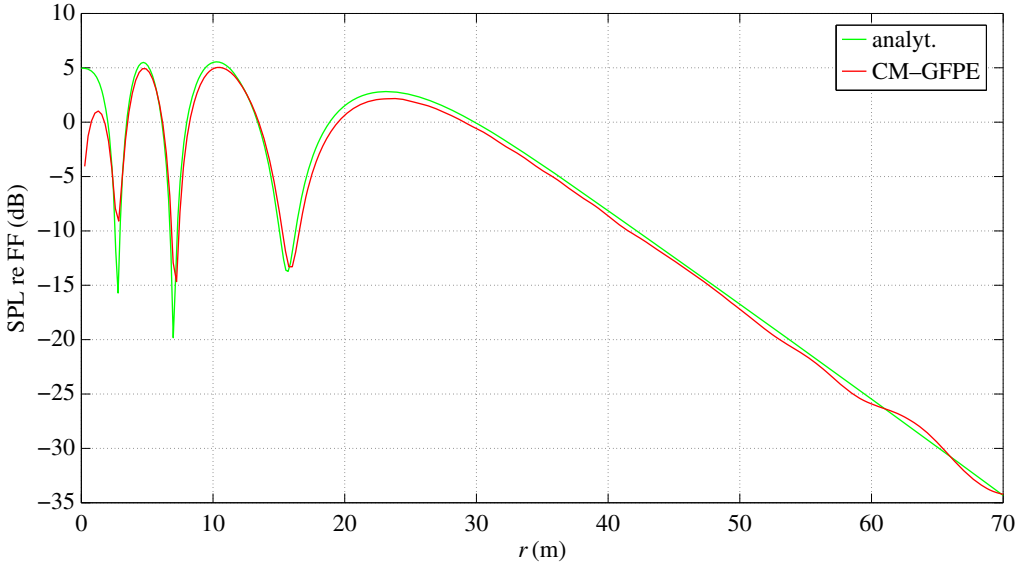


**Figure 4.** Sound pressure level (SPL), relative to free-field (FF) sound propagation, near a rigid convex circular cylinder at a fixed receiver height along the arc (validation case A). (Online version in colour.)

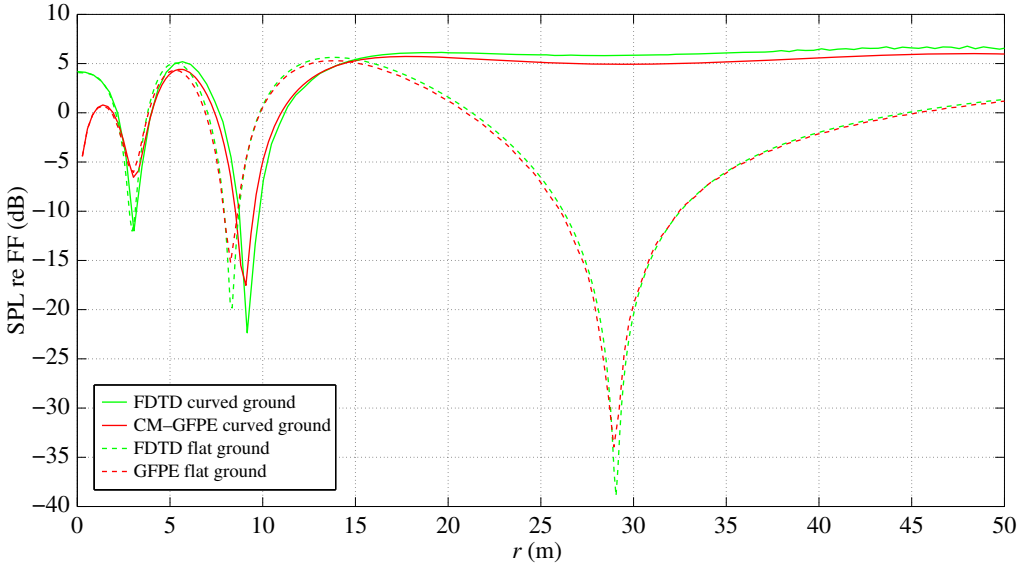


**Figure 5.** Sound pressure level (SPL), relative to free-field (FF) sound propagation, near a rigid concave circular cylinder at a fixed receiver height ('curved ground', validation case B) along the arc. For comparison, sound propagation over a flat rigid ground with the same source–receiver positioning is also depicted (flat ground). (Online version in colour.)

Figure 5 shows the comparison between the FDTD and the CM–GFPE methods for a concave rigid surface (validation case B). For comparison, sound propagation in the case of the same source–receiver geometry but over flat rigid ground is depicted. The specific curvature of the ground leads to some distinct effects, such as the loss of the strong destructive interference at about 29 m from the source, and the small shifts in interferences at short distance. The agreement between the FDTD and the CM–GFPE methods is very good, with differences smaller than 0.7 dB;

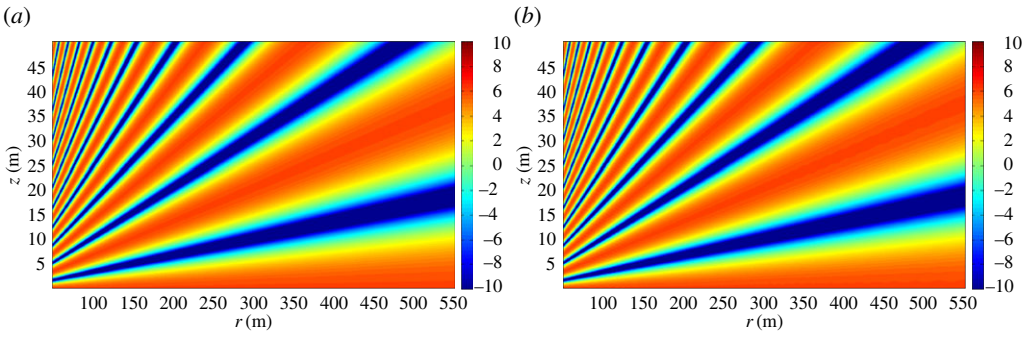


**Figure 6.** Sound pressure level, relative to free-field sound propagation (in dB), over flat rigid ground in a dense receiver grid. (*a*) GFPE results using an analytical starting field are depicted and (*b*) the (full) analytical solution (validation case C). (Online version in colour.)

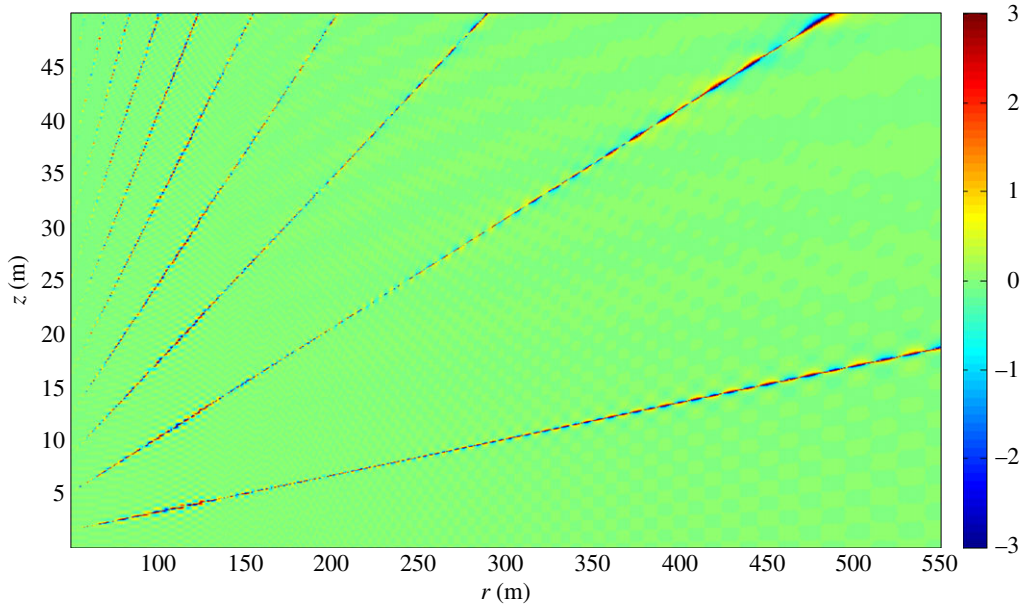


**Figure 7.** Sound pressure level difference (in dB) between GFPE predictions starting from an analytically constructed starting field and the full analytical solution for sound propagation over flat rigid ground (validation case C). (Online version in colour.)

similar remarks as for validation case A could be made regarding the angle limitation in PE close to the source, and regarding the magnitude of the destructive interferences. Other (small) differences might come from the fact that the FDTD is a full-wave technique, including backward scattering which is fully neglected in the forward-stepping GFPE approach, from the stair-step approach in FDTD, and from the fact that there will be small phase errors that are inherent to the FDTD technique [34]. Validation cases A and B further show the accuracy of the equivalence between a point source and coherent line source solutions in such complex geometries when expressing results relative to free-field sound propagation (see §2*a*).

Validation case C (figures 6 and 7) shows excellent agreement between the analytical solution applied to a dense receiver grid and the analytical starter propagated further with GFPE. The analytical starter is located at 50 m from the source. Only predictions from that distance on are depicted. The field plots presented in figure 6 are almost indistinguishable. The level differences

plotted in figure 7 show some small deviations only at the zones where the conditions for destructive interference are met.

## 5. Calculation example: valley ground type

This section shows the potential of the proposed hybrid analytical–CM–GFPE methodology to assess sound pressure levels across a valley in the case of a single ridge wind turbine. The influence of valley ground type is studied.

Sound propagating from a point source (concentrating all the wind turbine's emitted acoustic energy at hub height) at a height $z_s = 75$ m on top of the ridge is considered. The ridge part is rigid and has a radius $R_{c1} = 10$ m. Predictions are made across the adjacent valley with a radius $R_{c2}$ of 500 m at a fixed receiver height $z_r = 4$ m (i.e. the typical receiver height as used in noise mapping). Two valley ground types are modelled, namely rigid and grass-covered ground. For the latter, the common Delany & Bazley impedance model [35] has been used as being appropriate to model reflection from grassland and characterized by a flow resistivity of 200 kPa s m$^{-2}$.

The following numerical parameters were used for the simulations. An absorption layer [17] thickness of 150 wavelengths is chosen, with the ratio between d$r$ and d$z$ being set to 30. These choices are consistent with the guidelines presented in [26]. In order to sufficiently assess the sound field along the arc, and taking into account the strong (artificial) refraction to represent the ground curvature, 40 computational cells per wavelength were chosen in the vertical direction. As a result, the spatial step d$r$ stays below the wavelength. The starting field is constructed in detail up to 75% of the valley radius. No accuracy loss was observed by reducing the spatial sampling while calculating the starting field to five cells per wavelength, followed by linear interpolation. Part of a Hanning window was used to gradually allow the pressure to go to zero towards the top of the calculation domain in order to prevent spurious reflections. Analysis is performed in octave bands. Twenty sound frequencies were individually simulated with the hybrid analytical–CM–GFPE model to constitute each band.

Numerical results depicted in figure 8 show a rather complex sound pressure level distribution along the valley. In both ground type scenarios, significant shielding is observed directly near the source side of the valley. However, strong differences are predicted further across the valley. Starting from about the centre of the valley, near-free-field sound propagation is predicted at all octave bands for the rigid ground, while there is a much stronger reduction along the grass-covered valley. Effects become increasingly pronounced with increasing sound frequency, consistent with the fact that surface impedance decreases with frequency. These numerical simulations indicate the importance of ground type in the case of ridge wind turbines emitting sound into a valley. This behaviour deviates from wind turbine sound propagation above flat ground, where the effects of ground type are typically much less pronounced [36].

An estimation of the total wind turbine received sound pressure level is shown in figure 9, for both ground types. A (relative) spectrum is considered to allow balancing the importance of the different octave bands, as they behave quite differently during propagation across the valley. To perform this analysis, the mean over a large set of spectral source power level measurements near large horizontal-axis wind turbines with a power production of more than 2 MW, as reported in [15], is used. This spectrum is repeated in appendix B.

When assuming a total sound power level of 105 dBA, the 35 dBA broadband exposure level (i.e. −70 dBA in figure 9) below which negative noise-related effects are not expected (see Introduction) is predicted after 240 m (28°, relative to the interface between the ridge and valley segments) and 662 m (76°) propagation across the valley, for grass-covered and rigid ground, respectively. Note that these predicted distances involve a single wind turbine only; a series of wind turbines positioned on a ridge would be common practice, however.

Note that, in this assessment, the specific noise emission characteristics of wind turbines located on ridges is not included, neither are the complex wind fields that might be expected at such locations. In a strongly simplified approach, a logarithmic wind speed profile (homogeneous atmosphere) is assumed following the valley terrain, using an aerodynamic roughness length of

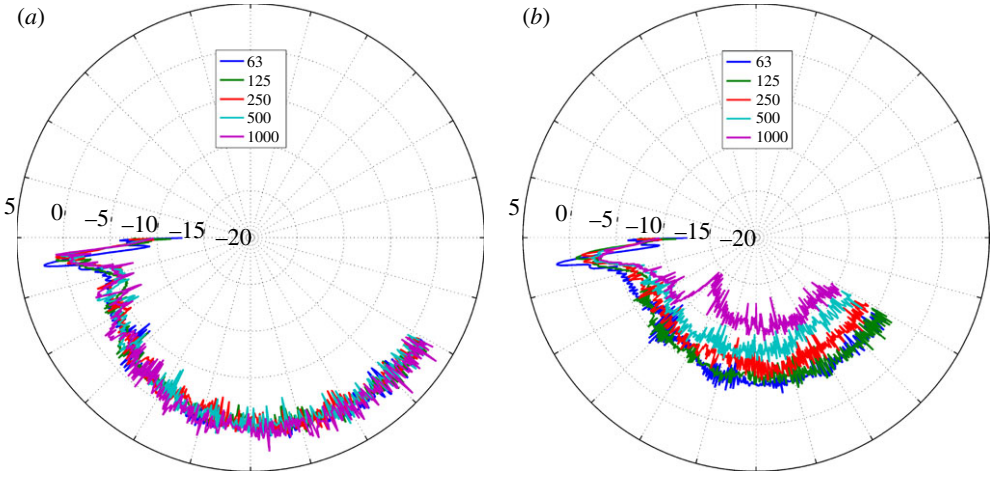


**Figure 8.** Predicted sound pressure levels (relative to free-field sound propagation, in dB) across the valley, in the case of a rigid (*a*) and a grass-covered valley (*b*), at a receiver height of 4 m. Octave bands with centre frequencies ranging from 63 Hz to 1 kHz are presented. (Online version in colour.)

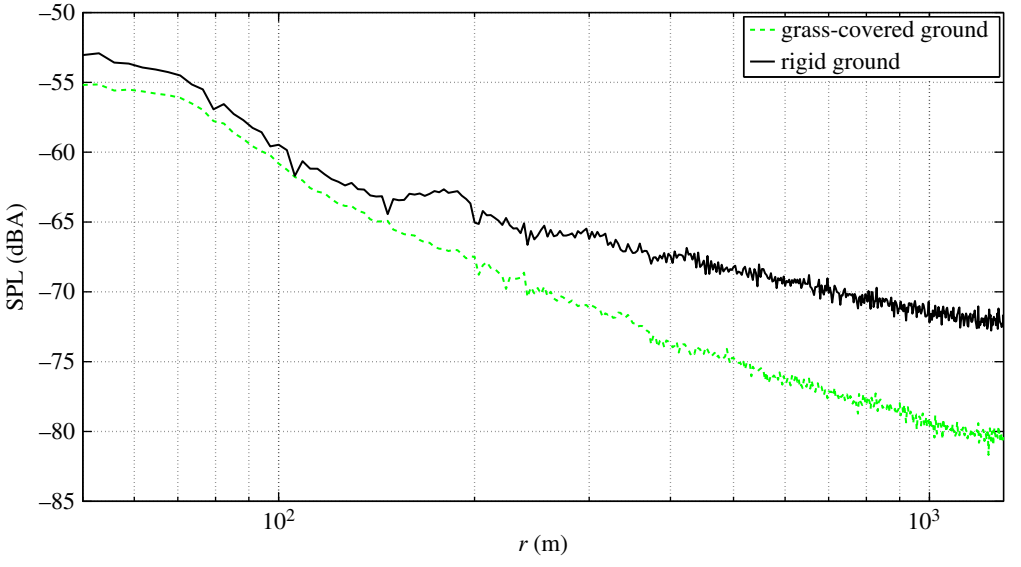


**Figure 9.** Predicted sound pressure levels (SPL) at a receiver height of 4 m across the valley arc, in the case of rigid and grass-covered valley ground. The total source power level is normalized to 0 dBA (see appendix B). (Online version in colour.)

0.05 m and a friction velocity of 0.4 m $s^{-1}$. Atmospheric absorption [37] is modelled assuming an air temperature of 10°C, a relative humidity of 70% and an atmospheric pressure of 101 300 Pa. The frequency range considered includes the octave band with centre frequency 2 kHz. For reasons of computational efficiency, the very time-consuming sound propagation calculations for the 2 kHz octave band were not performed (and the 1 kHz band results were recycled). This is justified by the fact that atmospheric absorption becomes pronounced at these higher frequencies and source power levels start to drop; a more accurate assessment of the propagation at this band would, therefore, only slightly increase accuracy when assessing total noise exposure levels from the wind turbine.

## 6. Conclusion

A hybrid analytical–CM–GFPE methodology is presented to model sound propagation from a ridge-mounted wind turbine, represented here by an elevated point source above the ridge, across an adjacent valley. The hybrid method relies on an analytical solution for sound diffraction around an impedance cylinder and the CM–GFPE technique. The geometry is simplified to a convex segment with a small radius, representing the ridge, followed by a large-radius concave circular segment, representing the valley. The hybrid model overcomes issues such as the unrealistic positioning of the source that would otherwise result from the CM approach, and the general angle limitation of the PE method. Various aspects of the model were successfully validated by means of cross-validations against other numerical or analytical techniques. Calculation examples show the complex sound pressure level distribution in such a ridge–valley geometry. At the source side of the valley, noise shielding from a (single) wind turbine is predicted. Starting from the centre of the valley, near-free-field sound propagation is observed at all octave bands for the rigid ground case, while there is a strong level reduction along a grass-covered valley. Although wind speed profiles were highly idealized in this work, the calculation methodology has the potential to include the effect of refraction and turbulent scattering as a result of the complex flow fields that might be associated with such a wind turbine placement.

Competing interests. I have no competing interests.
Funding. I received no funding for this study.
Acknowledgement. I am grateful to Dr Andrew Bullmore for proofreading the manuscript.

## Appendix A. Analytical solution for coherent line source diffraction around an impedance cylinder

The total pressure $p$ at point P, at a (radial) distance $R$ relative to the origin of the cylinder, emitted by a coherent line source at point Q, parallel to the cylinder axis and at a distance $R_\mathrm{q}$ from the origin of the cylinder, consists of the direct contribution from Q to P ($=p_\mathrm{d}$), and the scattered sound pressure ($=p_\mathrm{s}$) [33] (see figure 10):

$$p = p_\mathrm{d} + p_\mathrm{s}. \tag{A 1}$$

The direct contribution is calculated as follows (assuming a unity-amplitude source):

$$p_\mathrm{d} = H_0^2\left(k_0\sqrt{R_\mathrm{q}^2 + R^2 - 2R_\mathrm{q}R\cos(\theta)}\right). \tag{A 2}$$

Calculating the scattered field is somewhat more involved, and needs the following summation:

$$p_\mathrm{s} = \sum_{m=0}^{\infty} a_m \delta_m J_m(k_0 R_q) H_m^2(k_0 R)\cos(m\theta) \tag{A 3}$$

with

$$\delta_m = \begin{cases} 1, & m = 0, \\ 2, & m > 0. \end{cases} \tag{A 4}$$

The term $a_m$ in equation (A 3) is calculated as follows:

$$a_m = -\frac{\mathrm{i}J_m'(k_0 a) + (1/Z)J_m(k_0 a)}{\mathrm{i}H_m'^2(k_0 a) + (1/Z)H_m^2(k_0 a)}\frac{H_m^2(k_0 R_q)}{J_m(k_0 R_q)}. \tag{A 5}$$

The derivatives of the Bessel and Hankel functions, with respect to their arguments, can be calculated using the following expressions:

$$J_m'(k_0 a) = \frac{m}{k_0 a}J_m(k_0 a) - J_{m+1}(k_0 a) \tag{A 6}$$

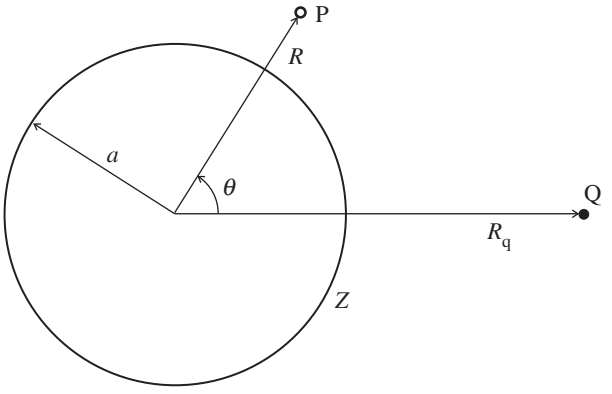


**Figure 10.** Overview of parameters involved in the analytical solution for coherent line source diffraction around an impedance cylinder.

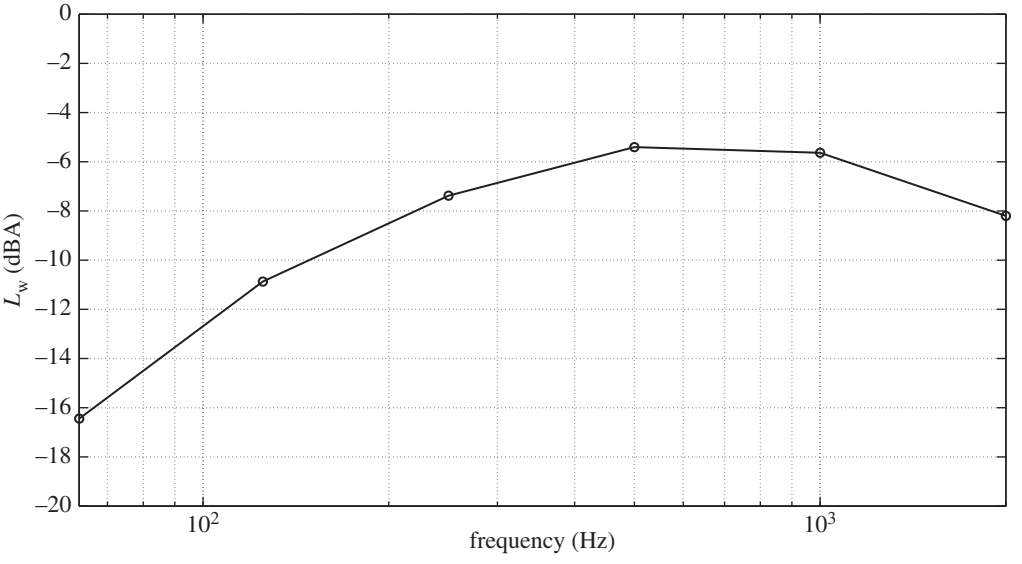


**Figure 11.** Source power level spectrum used for the calculations depicted in figure 9, based on Søndergaard [15]. The spectrum was normalized to a total source power level of 0 dBA.

and

$$H_m'^2(k_0a) = \tfrac{1}{2}(H_{m-1}^2(k_0a) - H_{m+1}^2(k_0a)). \tag{A 7}$$

In the equations above, $k_0$ is the wavenumber, $a$ the cylinder radius, $\theta$ the angle between source and receiver, $H_m^2$ the Hankel function of $m$th order and second kind, $J_m$ the Bessel function of order $m$ and $Z$ the (normalized) locally reacting surface impedance of the cylinder.

## Appendix B. Wind turbine source power spectrum

The source power level spectrum depicted in figure 11 was used to calculate total A-weighted exposure levels. This spectrum is the average based on a large number of measurements near horizontal-axis wind turbines with a power production of more than 2 MW, as reported by Søndergaard [15].

## References


1. Tabassum-Abbasi M, Abbasi T, Abbasi S. 2014 Wind energy: increasing deployment, rising environmental concerns. *Renew. Sust. Energy Rev.* **31**, 270–288. (doi:10.1016/j.rser.2013.11.019)
2. Kim H, Lee S, Son E, Lee S, Lee S. 2012 Aerodynamic noise analysis of large horizontal axis wind turbines considering fluid–structure interaction. *Renew. Energy* **42**, 46–53. (doi:10.1016/j.renene.2011.09.019)
3. Pedersen E, Waye K. 2004 Perception and annoyance due to wind turbine noise—a dose–response relationship. *J. Acoust. Soc. Am.* **116**, 3460–3470. (doi:10.1121/1.1815091)
4. Pedersen E, Waye K. 2007 Wind turbine noise, annoyance and self-reported health and well-being in different living environments. *Occup. Environ. Med.* **64**, 480–486. (doi:10.1136/oem.2006.031039)
5. Shepherd D, McBride D, Welch D, Dirks K, Hill E. 2011 Evaluating the impact of wind turbine noise on health-related quality of life. *Noise Health* **13**, 333–339. (doi:10.4103/1463-1741.85502)
6. Janssen S, Vos H, Eisses A, Pedersen E. 2011 A comparison between exposure–response relationships for wind turbine annoyance and annoyance due to other noise sources. *J. Acoust. Soc. Am.* **130**, 3746–3753. (doi:10.1121/1.3653984)
7. Bolin K, Nilsson M, Khan S. 2010 The potential of natural sounds to mask wind turbine noise. *Acta Acust. Acust.* **96**, 131–137. (doi:10.3813/AAA.918264)
8. Van Renterghem T, Bockstael A, De Weirt V, Botteldooren D. 2013 Annoyance, detection and recognition of wind turbine noise. *Sci. Total Environ.* **456–457**, 333–345. (doi:10.1016/j.scitotenv.2013.03.095)
9. Wharton S, Newman J, Qualley G, Miller W. 2015 Measuring turbine inflow with vertically-profiling lidar in complex terrain. *J. Wind Eng. Ind. Aerodyn.* **142**, 217–231. (doi:10.1016/j.jweia.2015.03.023)
10. Hunt J, Leibovich S, Richards K. 1988 Turbulent shear flows over low hills. *Q. J. R. Meteorol. Soc.* **114**, 1435–1470. (doi:10.1002/qj.49711448405)
11. Lemelin R, Surry D, Davenport A. 1988 Simple approximations for wind speed-up over hills. *J. Wind Eng. Ind. Aerodyn.* **28**, 117–127. (doi:10.1016/0167-6105(88)90108-0)
12. Lubitz W, White B. 2007 Wind-tunnel and field investigation of the effect of local wind direction on speed-up over hills. *J. Wind Eng. Ind. Aerodyn.* **95**, 639–661. (doi:10.1016/j.jweia.2006.09.001)
13. Evans T, Cooper J. 2011 Comparison of predicted and measured wind farm noise levels and implications for assessments of new wind farms. In *Proc. of ACOUSTICS 2011*, Gold Coast, Australia. See http://www.acoustics.asn.au/conference_proceedings/AAS2011/papers/p30.pdf.
14. Schmidt J, Klokker M. 2014 Health effects related to wind turbine noise exposure: a systematic review. *PLoS ONE* **9**, e114183. (doi:10.1371/journal.pone.0114183)
15. Søndergaard B. 2014 Noise and low frequency noise from wind turbines. In *Proc. of Internoise 2014*, Melbourne, Australia. See http://www.acoustics.asn.au/conference_proceedings/INTERNOISE2014/papers/p991.pdf.
16. Keith S, Feder K, Voicescu S, Soukhovtsev V, Denning A, Tsang J, Broner N, Richarz W, van den Berg F. 2016 Wind turbine sound power measurements. *J. Acoust. Soc. Am.* **139**, 1431–1435. (doi:10.1121/1.4942405)
17. Salomons E. 2001 *Computational atmospheric acoustics*. Dordrecht, The Netherlands: Kluwer.
18. Ostashev V, Wilson D. 2016 *Acoustics in moving inhomogeneous media*, 2nd edn. Boca Raton, FL: CRC Press.
19. Gilbert K, Di X. 1993 A fast Green's function method for one-way sound propagation in the atmosphere. *J. Acoust. Soc. Am.* **94**, 2343–2352. (doi:10.1121/1.407454)
20. Salomons E. 1998 Improved Green's function parabolic equation method for atmospheric sound propagation. *J. Acoust. Soc. Am.* **104**, 100–111. (doi:10.1121/1.423260)
21. Van Renterghem T, Salomons E, Botteldooren D. 2005 Efficient FDTD-PE model for sound propagation in situations with complex obstacles and wind profiles. *Acta Acust. Acust.* **91**, 671–679. See http://www.ingentaconnect.com/content/dav/aaua/2005/00000091/00000004/art00006/.
22. Sack R, West M. 1995 A parabolic equation for sound propagation in two dimensions over any smooth terrain profile: the generalised terrain parabolic equation (GT-PE). *Appl. Acoust.* **45**, 113–129. (doi:10.1016/0003-682X(94)00039-X)

23. Collins M. 1990 The rotated parabolic equation and sloping ocean bottoms. *J. Acoust. Soc. Am.* **87**, 1035–1037. (doi:10.1121/1.398829)
24. Bérengier M, Gauvreau B, Blanc-Benon P, Juvé D. 2003 Outdoor sound propagation: a short review on analytical and numerical approaches. *Acta Acust. Acust.* **89**, 980–991. See http://www.ingentaconnect.com/content/dav/aaua/2003/00000089/00000006/art00009/.
25. Van Renterghem T, Botteldooren D, Lercher P. 2007 Comparison of measurements and predictions of sound propagation in a valley-slope configuration in an inhomogeneous atmosphere. *J. Acoust. Soc. Am.* **121**, 2522–2533. (doi:10.1121/1.2717765)
26. Cooper J. 2003 Parameter selection in the Green's function parabolic equation for outdoor sound propagation over varied terrain. PhD thesis, Pennsylvania State University, USA.
27. Di X, Gilbert K. 1994 The effect of turbulence and irregular terrain on outdoor sound propagation. In *Proc. of the 6th Int. Symp. on Long-Range Sound Propagation*, Ottawa, Canada, pp. 315–333. National Research Council of Canada.
28. Li K, Wang Q, Attenborough K. 1998 Sound propagation over convex impedance surfaces. *J. Acoust. Soc. Am.* **104**, 2683–2691. (doi:10.1121/1.423852)
29. Defrance J *et al.* 2007 Outdoor sound propagation reference model developed in the European Harmonoise project. *Acta Acust. Acust.* **93**, 213–227. See http://www.ingentaconnect.com/content/dav/aaua/2007/00000093/00000002/art00005/.
30. Cooper J, Swanson D. 2007 Parameter selection in the Green's function parabolic equation. *Appl. Acoust.* **68**, 390–402. (doi:10.1016/j.apacoust.2006.02.008)
31. Botteldooren D. 1995 Finite-difference time-domain simulation of low-frequency room acoustic problems. *J. Acoust. Soc. Am.* **98**, 3302–3308. (doi:10.1121/1.413817)
32. Attenborough K, Li K, Horoshenkov K. 2007 *Predicting outdoor sound*. London, UK: Taylor and Francis.
33. Mechel F. 2008 *Formulas of acoustics*, 2nd edn. Berlin, Germany: Springer.
34. Van Renterghem T, Botteldooren D. 2007 Prediction-step staggered-in-time FDTD: an efficient numerical scheme to solve the linearised equations of fluid dynamics in outdoor sound propagation. *Appl. Acoust.* **68**, 201–216. (doi:10.1016/j.apacoust.2005.10.003)
35. Delany M, Bazley E. 1970 Acoustical properties of fibrous absorbent materials. *Appl. Acoust.* **3**, 105–116. (doi:10.1016/0003-682X(70)90031-9)
36. Sims J, Bullmore A, Van Renterghem T, Horoshenkov K. 2015 Wind turbine noise propagation—results of numerical modelling techniques to investigate specific scenarios. In *Proc. 6th Int. Conf. on Wind Turbine Noise*, Glasgow, UK. Institute of Noise Control Engineering.
37. ISO. 1996 *Acoustics—attenuation of sound during propagation outdoors—part 1*. ISO 9613-1:1996. Geneva, Switzerland: International Organisation for Standardisation.